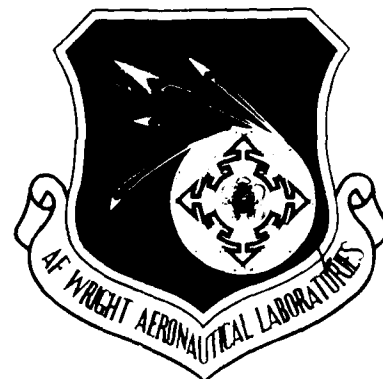AFWAL-TR-84-3070

STUDIES ON MIXING PROCESSES IN EJECTORS

A. KROTHPALLI
K. KARAMCHETI
B. G. McLACHLAN

KRETCH Inc.
450 San Antonio Road #46
Palo Alto, CA 94304

25 February 1985

November 1984

DTIC
SELECTED
JAN 1 4 1988
E

FLIGHT DYNAMICS LABORATORY
AIR FORCE WRIGHT AERONAUTICAL LABORATORIES
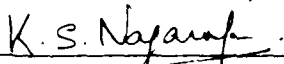AIR FORCE SYSTEMS COMMAND
WRIGHT-PATTERSON AFB, OHIO 45433-6553

K. S. Nagaraja

Aerospace Engineer
K. S. Nagaraja

FOR THE COMMANDER

ALFRED C. DRAPER, Acting Chief
Aeromechanics Division

Unclassified

SECURITY CLASSIFICATION OF THIS PAGE

REPORT DOCUMENTATION PAGE		Form Approved OMB No. 0704-0188

1a. REPORT SECURITY CLASSIFICATION Unclassified	1b. RESTRICTIVE MARKINGS

2a. SECURITY CLASSIFICATION AUTHORITY	3. DISTRIBUTION/AVAILABILITY OF REPORT Approved for Public Release; distribution unlimited.
2b. DECLASSIFICATION/DOWNGRADING SCHEDULE	

4. PERFORMING ORGANIZATION REPORT NUMBER(S) KRETECH TR 1	5. MONITORING ORGANIZATION REPORT NUMBER(S) AFWAL-TR-84-3070

6a. NAME OF PERFORMING ORGANIZATION KRETECH INC.	6b. OFFICE SYMBOL (If applicable)	7a. NAME OF MONITORING ORGANIZATION AFWAL/FIMM

6c. ADDRESS (City, State, and ZIP Code) 450 San Antonio Road # 46 Palo Alto, CA 94304	7b. ADDRESS (City, State, and ZIP Code) AFWAL/FIMM WPAFB, Dayton, Ohio 45433

8a. NAME OF FUNDING/SPONSORING ORGANIZATION	8b. OFFICE SYMBOL (If applicable) FIMM	9. PROCUREMENT INSTRUMENT IDENTIFICATION NUMBER F33615-82-C-3027

8c. ADDRESS (City, State, and ZIP Code) AFWAL/FIMM WPAFB, Dayton, Ohio. 45433	10 SOURCE OF FUNDING NUMBERS			
	PROGRAM ELEMENT NO 62201F	PROJECT NO. 2404	TASK NO 10	WORK UNIT ACCESSION NO 68

11. TITLE (Include Security Classification)

Studies on Mixing Processes in Ejector

12. PERSONAL AUTHOR(S)
A. Krothapalli, K. Karamacheti, and B.G. McLachlan

13a. TYPE OF REPORT Final Report	13b TIME COVERED FROM Aug 82 TO Nov 83	14. DATE OF REPORT (Year, Month, Day) November 15, 1984	15. PAGE COUNT 97

16. SUPPLEMENTARY NOTATION

17. COSATI CODES			18 SUBJECT TERMS (Continue on reverse if necessary and identify by block number)
FIELD	GROUP	SUB-GROUP	Ejectors, Performance, Thrust Augmentors. Mixing, Nozzle Exhaust Cooling, Turbulence.

19. ABSTRACT (Continue on reverse if necessary and identify by block number)

The capability of producing additional thrust along with the ability of vectoring the thrust makes the ejector an attractive device for V/STOL aircraft applications. In addition, the acoustic shielding provided by the walls of the shroud, and lowered exhaust velocities and temperatures at the ejector exit offer important advantages in the area of nozzle exhaust cooling. The present work was carried out because of the potential usefulness of ejectors for nozzle exhaust cooling. One of the physical processes which is known to play a large role on the performance of the total system is the mixing between the hot primary and cold secondary streams. Thus an attempt is made here to investigate the mixing process of a hot rectangular jet with an entrained cold ambient fluid in a simple form of a ejector.

For the primary nozzle, a convergent rectangular nozzle of aspect ratio of 10 was used. The Mach number at the nozzle exit was 0.3. The total temperature at the nozzle exit was varied from 20°C to 250°C. The area ratio (cross sectional area

20. DISTRIBUTION/AVAILABILITY OF ABSTRACT [X] UNCLASSIFIED/UNLIMITED ☐ SAME AS RPT ☐ DTIC USERS	21 ABSTRACT SECURITY CLASSIFICATION Unclassified
22a NAME OF RESPONSIBLE INDIVIDUAL Dr. K.S. Nagaraja	22b TELEPHONE (Include Area Code) 513-255-3439	22c OFFICE SYMBOL FIMM

DD Form 1473, JUN 86   Previous editions are obsolete.   SECURITY CLASSIFICATION OF THIS PAGE

of the rectangular duct/nozzle exit cross sectional area) was varied from 20 to 35.

Primary jet heating, over the temperature range tested, has no significant effect on the velocity field within the ejector shroud. The temperature decay within the ejector shroud displayed differences in comparison with the free jet up to a location where the primary jet spreads to the mixing duct wall. Downstream of this location the centerline temperature within the ejector is higher than that of a free jet.

A theoretical analysis is made to set up a determinate mathematical problem for the flow through a constant area ejector, in terms of parameters characterising the generation of the primary flow, the initial conditions from which the secondary flow is induced, and the conditions of the ambient medium. It is shown that multiple solutions (more than two) occur, and admissible ones out of these are those that fulfill the entropy condition.

Acknowledgements

Accession For	
NTIS GRA&I	☒
DTIC TAB	☐
Unannounced	☐
Justification	
By	
Distribution/	
Availability Codes	
Dist	Avail and/or Special
A-1	

DTIC
COPY
INSPECTED
3

TABLE OF CONTENTS

LIST OF FIGURES

TITLE

TITLE

1. INTRODUCTION

A thrust-augmenting ejector is a pneumatic device that utilizes a process in which a primary high speed jet is mixed with an entrained low speed secondary ambient stream in a duct to produce thrust greater than that of the primary jet when exhausted to ambient pressure. A simple ejector generally, consists of a primary nozzle and a shroud as shown in figure 1. The shroud can be a duct or a tube which consists of a contoured inlet section, a mixing duct and a diffuser. The primary nozzle is placed within the ejector shroud and expels high speed fluid. Concomitant with the mixing of the primary and secondary streams in the confined region is a reduction in the mean pressure which maintains the flow of the secondary stream through the inlet. The reduced pressure relative to the ambient acting on the inlet surfaces produces an additional force and it is this contribution which "augments" the primary jet force. The ratio of the force produced by the entire ejector system to the force produced by isentropically expanded primary jet to ambient pressure is generally called the thrust "augmentation ratio", and the ejector performance is most frequently characterized by this ratio.

The capability of producing additional thrust along with the ability of vectoring the thrust makes the ejector an attractive device for V/STOL aircraft applications. It is in this context several studies have been carried out during the last two decades. A review of the various facets of thrust-augmenting ejectors was recently given by Quinn[1] and Porter et.al[2], who also included references pertaining to the topic. In addition to the above, the acoustic shielding provided by the walls of the

1

shroud, and the lowered exhaust velocities and temperatures at the ejector exit offer important advantages in the area of nozzle exhaust cooling and infrared radiation from the jet.

The interest in the present work stems from the application of ejectors to nozzle exhaust cooling. If the entrainment and mixing of primary hot gas and cold ambient air are efficiently accomplished so that the desirable levels of cooling are achieved, while maintaining the thrust of the total system at approximately the same level as the primary jet or higher, the capability of the system is enhanced. It is therefore necessary to understand the physics of the mixing process as it affects the characteristics of the ejector exit flow.

One of the primary physical processes which is known to play a large role on the performance of an ejector is the mixing between the primary and secondary streams. Attempts have been made by several investigators to improve the mixing process through various types of nozzle designs, such as the hypermixing nozzle[3] and multiple jet nozzle[4] and by externally imposed oscillations of the primary jet[5]. Generally, most studies show improvements in performance when means are found to accelerate mixing between the primary and secondary streams. However, when the primary jet is heated, the mixing process that occurs between the hot jet and cold secondary flow in a confinement is poorly understood. Overall, the lack of understanding, both theoretical and experimental, of the details of the mixing process prevented the development of an efficient practical design of the ejector.

The object of the investigation reported in this paper is

2

not to devise an ejector which is new or excellent, but rather to test the utility and validity of using it to cool the nozzle exhaust. With this in mind, the overall objective of this investigation was to study the mixing process of a hot jet with entrained cold ambient fluid in a simple rectangular ejector which would perform in useful fashion.

It has been recognized recently that a rectangular (also called two dimensional) exhaust nozzle offers improved aircraft system performance as compared to an axisymmetric nozzle. Some of the benefits identified[6] for these nonaxisymmetric exhaust nozzles include: increased lift attributed to induced aerodynamics created by the nozzle exhaust flow near the wing trailing edge; and increased instantaneous maneuver with vectoring exhaust jet. With these advantages in mind, the present experiment utilizes a rectangular nozzle of moderate aspect ratio as a primary nozzle. The shroud used to simulate the ejector surfaces is also of rectangular cross section and consists of a contoured inlet section and a constant area duct as shown in Figure 3.

The specific objective of this experiment is to investigate the basic fluid mechanical properties, such as the mean and turbulence quantities, of a heated jet emanating from a rectangular nozzle into a confined region. The flow field of a heated rectangular jet issuing into quiet surroundings was found to have the characteristics of both two-dimensional jet and the axusymmetric jet. These two types of jets have been studied in some detail before; however, few experiments have been carried out on a rectangular jet with the degree of throughness found in

either of the above two cases. Therefore, one of the objectives of the present study is to investigate the characteristics of a heated rectangular free jet. This forms the first part of the present study. Although several experimental studies have been carried out to investigate the overall performance of various ejector configurations, very limited information exists in the literature on the detailed flow structure within ejectors. Recently some studies[7] have been carried out at Jet Propulsion Laboratories to study the entrainment and mixing in thrust augmenting ejectors using an unheated two dimensional primary nozzle. No information exists at this time on the effect of primary jet heating on the ejector flow structure, specifically using rectangular nozzles. In view of the objectives of the present investigation, there appears to be a need for fundamental studies concerning the turbulent mixing of a heated jet under confinement. This constitutes the second part of the present investigation.

In addition to the above experimental program a theorical analysis of the overall features of the flow through a constant area ejector, has been made. The detailed discussion of this analysis has been given in Chapter 5.

2. REVIEW OF PREVIOUS WORK AND NATURE OF THE PRESENT INVESTIGATION

The present study is comprised of two problems as identified in the introduction. Results of individual studies of these problems have been published in the literature in a form somewhat unrelated to one another. For the purposes of this review, it will be convenient to discuss separately the previous work in each topic. Comparisons will be made between the present and previous studies wherever possible.

2.1 HEATED RECTANGULAR FREE JET

Most of the previous investigations in heated turbulent jets were carried out on two dimensional jets and axisymmetric jets. A comprehensive list of references for the above two cases is given by Schetz[8]. Few experiments have been carried out on a heated rectangular jet with the degree of thoroughness found in either of the above two classes of jets. Early work on this subject was done by Higgins, et.al.[9], who measured mean velocity and temperature fields of rectangular jets for various jet exit Mach numbers. Their measurements show that the mean temperature and velocity along the center line of rectangular jets decay much more rapidly as compared to those of axisymmetric jets with equal exit areas. More recently, Sfeir[10], Sforza and Stasi[11] measured mean velocity and temperature fields of rectangular jets of various aspect ratios. Although they provided the data for both the mean and turbulent velocity fields of unheated jets, only the bulk properties are given for heated jets. These experiments revealed that the flow field of a heated rectangular free jet may be characterized, like in isothermal jet, by three

distinct regions defined by the decay of the mean axial velocity and temperature along the axis of the jet. Discussion of these regions are deferred to Chapter 4. It has also been pointed out that the nozzle inlet geometry and the nature of the exit flow conditions play a dominant role on the downstream development of the jet. Bobba and Ghia[12] attempted to calculate the flow field of a heated rectangular jet using the two-equation turbulence model consisting of those for the turbulent kinetic energy and its rate of dissipation, in terms of which the turbulence stresses are expressed. They were able to calculate some of the observed features. However, the lack of sufficient experimental data on the flow structure of hot jets limited the comparison of most of their results to an unheated case.

Systematic measurements such as those found for two dimensional jets, and axisymmetric jets, are not available for a heated rectangular free jet. There appears to be a need for additional data, in particular, measurements of turbulence quantities to further extend the understanding of its fluid mechanical characteristics. An attempt is made in the present investigation to provide some of these measurements for a hot rectangular free jet exiting from a nozzle of aspect ration 10. Results and discussion of these experiments are presented in Chapter 4.

2.2 HOT RECTANGULAR JET IN THE EJECTOR CONFIGURATION

Very few investigations have been carried out on ejector flows with the heated primary jets, and particularly, none on the detailed mixing characteristics of a confined heated jet. In trying to assess the dependence of the ejector performance on the

6

primary jet temperature Quinn[13] has conducted a systematic experiment, using an axisymmetric primary nozzle, at different pressure and temperature ratio ranging from 1.7 to 6.6 and 1.0 to 2.7 respectively. It has been observed that for a given pressure ratio the mixing between the primary and secondary streams is enhanced when the primary jet is hot and that this effect becomes more pronounced as the ratio of the length to width of the mixing duct is reduced. Most of the measurements obtained in the above investigation were aimed at measuring the gross characteristics of the flow field rather than the detailed structure of the flow. In addition, because of the limited attention given to jets issuing from rectangular nozzles, there is no known published information on the flow structure of a heated confined rectangular jet. Thus, there appears to be a need for a systematic study of mixing characteristics, of a heated confined jet. With this in mind we conducted the experiment described here. Results and discussion of the experiment are provided in Chapter 4.

2.3 NATURE OF THE PRESENT INVESTIGATION

The experimental studies mentioned above in addition to others, have contributed to a limited understanding of the characteristics of a heated free and confined rectangular jets. Very little is understood about the fundamental nature of the mixing phenomenon occuring between the primary and secondary streams under confinement. In the present study a methodical set of measurements were made of simple mean and turbulent quantities to evaluate the effects of confining surfaces on mixing of a

7

heated rectangular jet.

In the light of the previous experimental data the features
of the flow are expected to depend upon the following parameters:
the aspect-ratio of the nozzle, Mach number of the jet exit flow,
the Reynolds number, $Re=U_0 D/\nu$ at the exit of the nozzle, the
temperature ratio To/Ta, the inlet geometry of the nozzle, the
exit velocity profile, and conditions of the ambient medium into
which the jet is issuing. If the jet is confined, the following
additional parameters will also enter into the problem. Geometry
of the confining surfaces to simulate the ejector, area ratio and
duct length to width ratio.

A convergent rectangular nozzle of aspect ratio 10 was chosen
for the present study. The inlet geometry of the nozzle was
designed to obtain a flow with minimum disturbances at the exit.
A top-hat mean velocity and temperature profiles were obtained for
the conditions tested. An exit Mach number of 0.3 was chosen for
all the measurements reported. This results in a Reynolds number
of 3.4×10^4 based on the small dimension of the nozzle. The
ejector shroud consisted of a convergent streamlined inlet and a
constant area mixing duct, both having rectangular cross sections.
The area of the duct cross section could be varied by adjusting the
width of the duct. No diffuser was employed in the present study.
Hot wire anemonetry was used to make the velocity and temperature
measurements.

3. DESCRIPTION OF THE EXPERIMENT

3.1 GENERAL REMARKS

The flow structure within a rectangular jet ejector and the effect of primary jet heating on the flow structure was investigated. The experiments were performed in the jet facility of the Department of Aeronautics and Astronautics at Stanford University. Measurements were made of the mean velocity field, mean total temperature field, centerline rms velocity fluctuation, and ejector shroud surface pressure distribution. Schlieren flow visualization was also performed. In addition, measurements of the rectangular jet under free conditions (without the presence of the ejector shroud) were made as a basis for comparison.

The test facility, test conditions, data acquisition, and data analysis will be described in the sections to follow.

3.2 TEST FACILITY

Model (Nozzle and Ejector Shroud)

The configuration tested, primary jet nozzle and ejector shroud, is shown in Figures 2 To 4. The rectangular primary jet nozzle is of aspect ratio 10 (L = 50 mm, D = 5 mm). The nozzle lip thickness is 1.7 mm. The nozzle exit is preceded by a 40 mm long rectangular (50 x 5 mm) channel. The ejector shroud consists of a contoured inlet and a 50-cm long constant area mixing duct of rectangular cross section. One dimension of the duct cross section (H) is fixed at 7 cm. The other dimension (W) is adjustable between 4 to 12 cm. The ejector shroud is made of plexiglas. The two duct walls parallel to the short dimension of

the nozzle can be replaced by optical glass windows for flow
visualization.

Air Supply System

The air supply system is of the blow down type. A spherical
compressed air storage tank (2.9 cu. m) provided the air flow to
a cylindrical settling chamber, 1.75 m in length, and 0.6 m in
diameter. The air, before reaching the nozzle, was passed
through an adapter containing six screens set 5 cm apart to
reduce disturbances at the nozzle inlet. For the heated jet
tests the settling chamber air temperature was increased a
selected amount above the ambient (room) temperature by
resistance heating elements placed in the air line from the
storage tank to the settling chamber. An iron-constantin ther-
mocouple placed just downstream of the adapter screens was used
to monitor the air temperature in the settling chamber. The
settling chamber air temperature was found to be identical to the
nozzle exit total temperature. For the heated jet tests the air
temperature was maintained to an accuracy of $\pm 1.0^\circ$ C. For a
detailed description of the facility see Hsia et. al[14].

Traversing Mechanism

The velocity and temperature probes were mounted on a sting
support, parallel to the jet axis and 50 cm in length which
itself was attached to a traversing mechanism. The traversing
mechanism provided translational motion along three orthogonal
axes. Each axis was aligned parallel to one of the nozzle co-
ordinate axes (see Figure 2). Stepper motors drive the two

10

horizontal axes lead screws; an analog motor drives the vertical axis lead screw. The horizontal axes (Y and Z) incorporate an electrical output voltage proportional to probe position. This allowed direct plotting of velocity and temperature levels versus position on an X-Y plotter.

3.3 TEST CONDITIONS

In the present study the primary jet exit Mach number (M_o) was held constant at 0.3. The duct width ratio (W/D) varied from 24 to 16. Two primary jet temperature conditions were studied, isothermal and heated, corresponding to jet exit total temperatures (T_o) of 20^oC room temperature and 85^oC, respectively.

Measurements were made with the ejector primary jet issuing vertically into the essentially still air conditions of the laboratory. Mean velocity and total temperature traverses *were made in the two central (X-Y, X-Z) planes at various streamwise locations* (X) up to 92D. Continuous profiles were made across the entire jet in order to establish symmetry of the flow about its central planes. However, only data for each half-plane will be presented.

3.4 DATA ACQUISITION (INSTRUMENTATION)

Static Pressure

Static pressure holes (.013 in. dia.) were distributed in six longitudinal rows over the four interior walls of the ejector shroud. These six longitudinal rows are indicated in Figure 4 by Roman numerals.

A conventional Scanivalve system (four type 'J' 24 port units) was used to measure the static pressure. The Scanivalve

11

pressure transducer (Gould model PM131TC, range +2.5 psid)
signals, after passing through signal conditioners (B&F model 1-
700SG), were amplified (Neff type 126) and sent to the analog/
digital interface of a computer (PDP 11/23) for storage and
analysis. The computer (PDP 11/23) provided control of the
Scanivalve units. At each measurement point, after a 150 msec
settling time, 30 samples over a 30 msec time interval were
obtained. The 30 sample average being calculated and stored on
the computer.

The Scanivalve pressure transducers were statically cali-
brated and adjusted to provide +10 volts/psig. Each pressure
transducer calibration curve was found to be linear.

Velocity

Velocity measurements were made with a single channel hot-
wire anemometer with linearizer (DISA 'M' series). A temperature
compensating bridge (DISA 55M14) was employed in the anemometer
to compensate for the temperature fluctuations in the heated jet
environment. A parallel array hot-wire probe (DISA 5P71) was
used for the measurements. This probe is constructed of two 5 mm
platinum plated tungsten wires, with an active length of 1.2 mm,
mounted parallel .4 mm apart on straight prongs. One wire is the
velocity sensor, the other wire is connected to the opposite arm
of the bridge, and provides dynamic compensation of temperature
fluctuations in the flow. All velocity measurements were made
with the probe wires parallel to the long dimension of the nozzle
(i.e. the Z axis). The linearized bridge output voltage was sent
to a TSI 1076 digital voltmeter and DISA 55D35 rms voltmeter, for

12

mean and rms values, respectively. The mean and rms values were recorded manually.

Hot-wire calibration was performed in the low turbulence air jet produced by a hot-wire calibrator (DISA 55D90). The hot-wire was linearized over a velocity range of 0 to 100 m/s.

As a check of the hot-wire data, a total pressure survey was made along the centerline of the free jet under heated and isothermal conditions. The total pressure probe (a hypodermic needle) was connected to one transducer of the Scanivalve unit used in the ejector shroud static pressure survey.

Temperature

The mean total temperature field was measured using a single channel constant current anemometer (DISA 5M01 main unit with a DISA 5P11), operated as a resistance thermometer, was used for the measurements. This probe is constructed of 5 mm diameter platinum plated tungsten wire with an active length of 1.2 mm. For the measurements the hot-wire was oriented parallel to the Z axis. The bridge output voltage was recorded manually from a DC voltmeter (TSI 1076).

By nature of the circuitry the bridge output voltage is a linear function of temperature. The calibration curve, bridge output voltage as a function of temperature, was determined by placing the wire sensor (sealed in a test tube of small volume) in a container of heated water that was at a stable defined temperature. For the measurements, a probe current of .2 mA was used. It was verified, by placing the probe in a hot-wire calibrator (DISA 55D90) air jet, that (over the test velocity range)

13

the probe resistance (and thus the bridge output voltage) was independent of velocity.

Flow Visualization

The Schlieren method was used for flow visualization. The Schlieren set-up was of single pass design, the optical axis folded twice, using two-25 cm diameter 3.05-m focal length spherical mirrors. The light source employed was a stroboscopic high intensity flash unit (U.S. Scientific Instruments Model 3015 stroboscope). The light source was triggered manually to produce a single flash of 1.5 sec duration for photographic record. Polaroid type 57 high speed film (ASA 3000) was used. The stroboscope feature of the light source was used for visual observation of the jet flow field.

3.5 DATA ANALYSIS

The ejector shroud wall static pressure survey data were processed into engineering units and coefficient form using a computer (PDP 11/23). Data from the static pressure measurements was converted into coefficient form using the conventional scaling

$$Cp = (P - Pa)/q$$

where
Pa = ambient pressure
q = primary jet exit dynamic pressure.

The duct wall static pressures presented in the text are the average of the values from the 'suction peak' that occurs at $X/D = 0$ (refer to Figure 4). All the duct wall static pressures from each longitudinal array are presented individually in Appendix A.

14

As stated previously a total pressure survey was made along the free jet centerline, under heated and isothermal conditions, as a check of the hot-wire velocity survey data. The measured total pressures were converted to mean velocity directly using the incompressible form of the Bernoulli equation (assuming the mean static pressure was ambient, with no correction for turbulent fluctuations). Excellent agreement is shown between the total pressure and hot-wire probe mean velocity values; this agreement is displayed in Figure 5 where the jet centerline mean velocity, normalized with respect to the jet exit mean velocity, is plotted as a function of streamwise location (X/D).

4. RESULTS AND DISCUSSION

4.1 FLOW VISUALIZATION

Schlieren flow visualization was performed to qualitatively assess the ejector flow field development. Representative schlieren photographs are displayed in Figure 6. The photographs cover the X-Y plane of the flow field from $X/D = 3$ to 40. The schlieren knife edge is vertical. Flow visualization revealed that the presence of the ejector shroud reduces jet spreading for isothermal and heated conditions (see Figure 6a). However, in the presence of the ejector shroud the jet spreading is not significantly affected by heating (See Figure 6b) and duct width (see Figure 6c) for the conditions tested.

The observation of a reduction in jet spreading due to confinement was also made in the two-dimensional ejector study of Bernal et al.[7]. It is known[15] that the presence of a co-flowing stream reduces two-dimensional jet growth. Hence, Bernal et al.[7] attributed this reduction to jet spreading to the presence of the co-flowing stream in the ejector, i.e. the secondary flow.

4.2 EJECTOR SURFACE STATIC PRESSURE CHARACTERISTICS

The affect of heating and duct width on the ejector shroud surface static pressure distribution is displayed in Figure 7. The typical static pressures presented are the average of the values from the longitudinal array of pressure taps from locations III to VI shown in Figure 4. At a fixed duct width the static pressure decreases through the contoured inlet, to a minimum at the contoured inlet end (i.e. the flow accelerates), and increases in the constant area mixing duct (i.e. the flow

16

decelerates). As the duct width increases the static pressure increases. Primary jet heating, for a given duct width, results in a slight static pressure decrease. Downstream of the contoured inlet the difference between the heated and isothermal static pressure distributions increases as the duct width decreases. This difference is greatest in the region $\overline{X}/D = 10$ to 60. It is in this region that the mixing between the primary and secondary flow takes place.

Of note in Figure 7, at a fixed duct width, is a change in gradient of the static pressure distribution at $\overline{X}/D = 60$. This same behavior has been noted in axisymmetric[13] and two-dimensional[7] ejector studies. It is suggested that this gradient change is due to the primary jet reaching the mixing duct wall. This conclusion is supported by the velocity field results of the present test and those of Bernal et.al.[7].

Since the mixing duct is of constant cross section the thrust due to the ejector shroud arises from the pressure distribution over the duct contoured inlet (refer to Figure 3). Therefore, at a fixed duct width, the minimum pressure value, Cp_{min}, that occurs at the end of the contoured inlet ($\overline{X}/D = 0$) is an indicator of the thrust due to the ejector shroud. Figure 8 shows the variation of Cp_{min} for three different area ratios and for two different nozzle exit temperatures. As suggested from Figures 6 and 7, that as the duct width increases, the minimum static pressure increases in a manner shown in the figure. Also observed from the figure that Cp_{min} slightly decreases as the primary jet exit total temperature increases.

Because of the three dimensional nature of the flow field

17

inside the duct, surface pressure measurements were made in different planes (see figure 4), and for different area ratios. These detailed surface pressure plots are presented in Appendix A.

4.3 MEAN VELOCITY AND TEMPERATURE FIELDS

Plotted in Figure 9, for heated conditions, is the square of the mean velocity along the ejector centerline as a function of downstream location. Also plotted in Figure 9 are the free jet results. At a fixed primary jet exit total temperature the affect of confinement is to increase the centerline mean axial velocity. This observation is consistent with the flow visualization results: namely, confinement reduces jet spreading. The isothermal jet results showed (Figure 10), at corresponding locations, the same velocity change increment due to confinement. The different slopes indicated in these plots are generally observed in the development of a free rectangular jet as will be shown below.

On the basis of the present investigation and the results reported by Sfeir[10] and Sforza and Stasi[11], the flow field of a free rectangular jet may be represented schematically as shown in Figure 11. The three regions identified in the figure may be defined as follows: the first region is referred to as a potential core region in which the axial component of velocity is essentially a constant; the second region marked by AB in which the velocity decays at a rate roughly the same as that of a planar jet, will be referred to as the two-dimensional region; and the third region, downstream of B, in which the velocity

decays at nearly the same rate as that of an axisymmetric jet, will be referred to as an axisymmetric region. The two dimensional type region originates at about the location where the two shear layers in the X,Y plane meet. Correspondingly, one may expect the axisymmetric region to originate at the location where the two shear layers in the X,Z plane would meet. The temperature field is also found to be divided in three distinct regions as described above. However, those regions are not exactly the same for temperature as for velocity, the former being shifted somewhat upstream of the latter.

Figure 12 shows, for a nozzle of aspect ratio 10, the measured decay of the square of the axial mean velocity along the center line for both isothermal and heated jets. The three regions introduced in Figure 11 are noted as the potential core region which ends at approximately 4D, the two dimensional jet type region extending up to about 40D, and the axisymmetric jet type region extending beyond 40D. The velocity data for both the isothermal and heated cases are seen to be identical, except for the lower normalized velocities for the heated case. Similar observations were also made by Storza and Stasi[11].

Similar to the observations made in a free jet, for the confined jet the effect of primary jet heating results in a decrease in the center line mean velocity, at corresponding down stream locations, as shown in Figure 13 of the case of the confined jet (W/D = 24). The same velocity decrease increment was displayed, at identical locations in the free jet results (see Figure 12). The center line velocity data for the confined jet do not display the two distinct regions beyond the

19

potential core. We suggest that in the presence of a uniform stream, the transition point (B in Figure 11) between the two dimensional region and the axisymmetric region may appear much farther downstream as compared to the corresponding free jet.

Figure 14 shows the centerline mean total temperature excess as a function of downstream location for free/confined conditions. The centerline mean total temperature for the confined jet is almost identical to the free jet up to X equal to 50D. The flow visualization and the velocity profiles show that the jet reaches the wall approximately at $X/D = 50$. For X greater than 50D the mean total temperature of the confined jet is higher than that of the free jet at the same location. The three regions noted above can also be observed in this plot.

Jet spreading in the two central planes is illustrated in Figures 15 to 17. The half-width is defined as the distance from the jet centerline to the point where the mean axial velocity or total temperature excess in each plane is equal to one-half of its centerline value.

The velocity half-widths are shown in Figure 15. In the X-Y plane the free jet spreads linearly with X. In the X-Z plane the velocity half-width remains approximately constant and then increases. At some intermediate location the half-widths from the two central planes cross over. Initially the confined jet (Figure 16) also spreads linearly with X up to X/D equal to 60. Beyond that point the confined jet spreading is reduced. This indicates that the jet has reached the mixing duct wall at about

20

that location. Note that the confined jet spreading is reduced in comparison to the free jet. Primary jet heating has little ffect on this behavior for both free and confined conditions.

The temperature half-widths are shown in Figure 17. In the temperature half-widths display the same qualitative behavior as found in the velocity half-widths. However, the crossover point for the free jet temperature half-widths is slightly upstream of the crossover point for the velocity half-widths. In addition, the free jet temperature half-widths are greater than the velocity half-widths. Similar observations have been noted in the heated free rectangular jet studies of Sforza et.al[11] and Sfeir[10]. The confined jet temperature and velocity half-widths exhibit no significant differences.

Jet development is further illustrated in the mean velocity and total temperature profiles of Figures 18 to 21. The profiles were plotted with an X-Y recorder with the averaged (time constant = 1 sec) single normal wire probe output connected to the Y axis while the probe position was displayed on the X axis. The plots are to scale. Since primary jet heating had negligible affect on the velocity field only the isothermal jet velocity profiles are presented.

Confined jet velocity profiles, in the two central planes, are shown in Figure 18. In the central X-Y plane velocity pro-files, the primary and secondary flow are mixing at X/D equal to 60: an indication that the jet has spread to the mixing duct wall at that location. This is confirmed in the confined jet velocity half widths (Figure 16). In the central X-Z plane velocity profiles, the jet appears to have spread to the mixing

21

duct wall by X/D equal to 20. Just upstream of the mixing duct exit (i.e. at X/D = 92) the central X-Z plane velocity profile is uniform, indicating complete mixing, and the central X-Y plane velocity profile is non-uniform, indicating incomplete mixing. Bevilaqua[3] has shown that ejector performance (i.e. thrust augmentation) is proportional to the degree of mixing achieved at the ejector exit. Of note, is that there is a noticeable amount of secondary flow in the X-Y plane profiles (e.g. X/D = 10 profile). The ratio of secondary flow velocity (jet exit velocity) is about .15.

Except for the secondary flow the confined jet velocity profiles in the X-Y plane look similar to those of the free jet (Figure 19). Far downstream the free jet velocity profiles in the X-Z plane are not uniform due to the absence of wall effects.

The confined jet temperature profiles are displayed in Figure 20 and exhibit characteristics similar to the velocity profiles (Figure 18): a gaussian shaped profile in the X-Y plane, and a nearly flat profile in the X-Z plane. Except for wall effects in the X-Z plane, the confined jet temperature profiles look similar to those of the free jet (Figure 21).

Evident in the confined and free jet nozzle exit X-Z plane temperature profiles (Figures 20, 21) are sharply defined inverted "spikes" near the ends of the jet. The "spikes" disappear downstream. Such "spikes" have not been noted in the temperature field measurements of the heated free rectangular jet studies[10, 11] that exist in the literature. It is interesting to speculate that they may be linked to the nozzle inlet geometry:

nozzle inlet geometry has been shown[16,17] to influence the velocity field of isothermal rectangular jets, especially the near velocity fi... However, at present the cause of the "spikes" is unkn...

Figure 22 shows the distribu... n of mean velocity across the free jet in the X,Y plane at diff... ent downstream stations, ranging from 20 to ?2 widths for both i... thermal and heated jets. The velocity is n...malized with res[... to U_c at each station, while the distanc... Y is normalized ... he distance X to the station in question. ...or both condition... ested the profiles are geometrically similar, within the limits of error for the experiment, for X greater than ... equal to 4... The shape of the profiles for isother...l a...i he...ted jet s... to be quite similar. From these observations it ...ppears th... for the conditions tested, heating does not p'ay a critical ro... in determining the shape of the similarity pr)file.

Normalized mean velocity profiles in the X, Z plane for different downstream locations are shown in Figure 23. The distance Z is again nomalized with respect to the local longitudinal distance. When compared at corresponding locations, the profiles for isothermal and heated jets seem to be similar.

4.4 R.M.S. INTENSITIES

The rms values of the velocity on the center line of the jet, for both free and confined configurations are shown in Figures 24 to 26. The magnitudes of the rms values for the heated jet case should be treated with some care because of the large errors involved. However, the overall trends of the data

23

can be expected to be quite correct. In Figure 24, the rms values are normalized with respect to the local mean velocity on the center line. For X greater than 30D, a substantial reduction in the nomralized values for the confined jet, as compared to the free jet, is noticed. Heating does not have a significant effect on the variation of rms values. Such reduction in turbulence intensities for a confined jet can also be observed in the data of Bernal et. al[7]. The behavior of the data for the free jet is typical of a rectangular jet (see for example Krothapalli et.al[4]).

To study the variation of absolute rms values with down-stream distance, these values are normalized with respect to the nozzle exit mean velocity, and are shown in Figure 25 and 26 for free and confined jet respectively. Figure 25 shows that the magnitude of the normalized rms velocity increases sharply close to the jet exit and reaches a maximum value at X equal to 10D. It then decreases monotonically as shown. Such a behavior is also observed for the confined jet (Figure 26), except when compared at a corresponding location, the magnitude of the r.m.s velocity is lower than that of a free jet. From these observations it is suggested that the presence of the secondary flow in the ejector duct reduces the turbulence intensities in the jet. And for the conditions tested heating has very little influence on the magnitude and variation rms intensities.

AN ALTERNATIVE FORMULATION OF THE CONSTANT AREA EJECTOR

An analysis only is presented in the following section. The approach to the mathematical development of the ejector flows is quite general and does not require specifying certain thermodynamic quantities for initiating the solution process at the ejector inlet.

5. APPROXIMATION ANALYSIS OF THE OVERALL FEATURES OF THE FLOW
THROUGH A CONSTANT AREA EJECTOR

5.1 INTRODUCTION

The objective of the analytical study of the present contract is to examine the nature of the dependence of the overall characteristics of the flow through a constant area ejector on the parameters governing the flow. For this purpose, an approximate analysis based on a determinate mathematical formulation is sought. The flow consists of a primary jet issuing into a constant area duct which follows an initially converging duct, and an induced secondary flow into the duct. The section containing the jet exit is the inlet section where the primary and secondary flows begin to mix. The fully mixed flow discharges at the outlet section into the ambient atmosphere. What is required is a determinate formulation in terms of the parameters characterizing the generation of the primary flow, the initial conditions from which the secondary flow is induced, and the conditions of the ambient medium.

In previous investigations the analysis is carried out by specifying the inlet conditions such as the Mach numbers and the stagnation temperatures of the primary and secondary flow respectively. It is, however, not clear, a priori, how a determinate problem is posed. In the present analysis attempt is made first to set up a determinate problem and then to determine the inlet and outlet conditions of the flow. It is shown that multiple solutions are likely to occur. Admissible ones out of these are those that fulfill the entropy condition. Expressions

for determining the required flow quantities are given in non-dimensional form in terms of the non-dimensional parameters characterizing the problem. The approach given here can be readily extended to more complicated flow situations such as those involving different primary and secondary fluids and chemical and non-equilibrium processes.

5.2 FORMULATION OF THE PROBLEM

We consider the steady flow of a fluid through an ejector configuration illustrated in the fig. 1a on p. 51. A jet issues from a nozzle into a region enclosed by a rigid imper-meable duct (ejector duct) which, initially, is of converging cross section and thereafter is of constant cross section extending over a finite length. We refer to the flow through the nozzle at its exit as the primary flow; the flow induced in the converging duct of the ejector as it appears at the cross section containing the primary nozzle exit as the secondary flow; the flow exiting from the ejector as the mixed flow. The flow cross section containing the nozzle exit will be referred to as the inlet section while the ejector exit section as the outlet section.

Basic Equations

The starting point for an approximate analysis of the overall features of the flow is the system of basic equations of fluid motion formulated in the integral form on the basis of a fixed region R in space enclosed by a surface S. In applying these equations to the ejector flow we chose the region R as that enclosed by the inlet and exit sections and the ejector duct wall between those sections and assume the following:

No frictional effects at the duct wall, no heat flow through the wall.

The effects of heat flow and friction at the inlet and outlet sections can be neglected.

However, the effects of friction and heat flow resulting in entropy production in the region R should be properly taken into account so as to ensure the satisfaction of the law of entropy.

The primary, secondary and the mixed flow fluids are simple thermodynamic fluids, that is any two thermodynamic variables are adequate to specify the thermodynamic state of the fluid.

The fluid properties in the primary, secondary, and mixed flows are uniform across their respective cross sectional

28

areas.

The velocities of the primary, secondary
and mixed flows are given respectively
by

$$\overrightarrow{V}_{\emptyset} = u_{\emptyset} \; \overrightarrow{e}_x$$

$$\overrightarrow{V}_1 = u_1 \; \overrightarrow{e}_x$$

$$\overrightarrow{V}_2 = u_2 \; \overrightarrow{e}_x$$

Where, $\overrightarrow{e}_x$, as shown in the fig. on p. 27 is the
direction of the ejector axis from the
nozzle exit towards the outlet section.
The duct wall is rigid and impermeable
and, therefore, the normal (to the wall)
component of fluid velocity at the wall
is zero.

We now introduce the following notation to denote the
various quantities (see the Figure on p. 27)

Flow	Flow		
quantity	Primary	Secondary	Mixed
speed	$u_{\emptyset}$	u_1	u_2
density	$\rho_{\emptyset}$	ρ_1	ρ_2
pressure	$p_{\emptyset}$	p_1	p_2
enthalpy	$h_{\emptyset}$	h_1	h_2
entropy	$s_{\emptyset}$	s_1	s_2
flow cross-section	$A_{\emptyset}$	A_1	A_2

With the use of this notation and the assumptions enumerated

29

above (assuming further that no other flow processes such as chemical reactions are present) the basic equations may be expressed as follows:

Equation of mass:

$$\rho_0 u_0 A_0 + \rho_1 u_1 A_1 = \rho_2 u_2 A_2 \ . \tag{1}$$

Equation of momentum:

$$(p_0 + \rho_0 u_0^2)A_0 + (p_1 + \rho_1 u_1^2)A_1 = (p_2 + \rho_2 u_2^2)A_2 \ . \tag{2}$$

Equation of energy:

$$\rho_0 (h_0 + \frac{u_0^2}{2})u_0 A_0 + \rho_1 (h_1 + \frac{u_1^2}{2})u_1 A_1 = \rho_2 (h_2 + \frac{u_2^2}{2})u_2 A_2 \ . \tag{3}$$

Equations of state:

$$h_0 = h_0(p_0, \rho_0) \ , \tag{4}$$

$$h_1 = h_1(p_1, \rho_1) \ , \tag{5}$$

$$h_2 = h_2(p_2, \rho_2) \ . \tag{6}$$

Entropy condition according to the law of entropy

$$\rho_2 u_2 S_2 A_2 - (\rho_0 S_0 u_0 A_0 + \rho_1 S_1 u_1 A_1) > 0 \ . \tag{7}$$

Here

$$S_0 = S_0(p_0, \rho_0) \ , \tag{8}$$

$$S_1 = S_1(p_1, \rho_1) \ , \tag{9}$$

$$S_2 = S_2(p_2, \rho_2) \ . \tag{10}$$

We note that there are twelve unknowns, namely

$$(\rho_0, p_0, h_0, u_0); (\rho_1, p_1, h_1, u_1); \text{ and } (\rho_2, p_2, h_2, u_2) \ .$$

However, at this stage, there are only six equations, namely (1), (2), (3), (4), (5) and (6) to solve for them. Additional equations are needed. They are developed as discussed below. The entropy condition (7) determines the admissible solutions for the unknowns.

With the intent of providing additional relations between the unknowns one may assume that two tangential (or vortex-sheet) discontinuities occur in the flow: one, at the lip boundary of the nozzle exit, between the primary and secondary flows; and another, at the lip of the ejector exit section, between the mixed flow and the ambient fluid. Then, according to the conditions of tangential discontinuity we require that

$$p_0 = p_1 \tag{11}$$

and

$$p_2 = p_a \tag{12}$$

where p_a is the <u>specified</u> pressure of the ambient fluid at the ejector exit lip. We note that the required velocity conditions at these discontinuities are fulfilled in light of the assumptions with regard to the velocities $\vec{V_0}$, $\vec{V_1}$, $\vec{V_2}$ and the velocity of the ambient fluid being zero or parallel to $\vec{e_x}$.

It is important to note that the assumption of such discontinuities is reasonable only if the flows involved are all subsonic. If the primary flow is choked or if one or the other flows is supposed to be supersonic, the above relations (11) and (12) expressing pressure continuity cannot be asserted, since in such cases, the adjustment between the different regions of flow will involve, in general, expansion waves, normal or shock discontinuities and probably tangential discontinuities. Analyses of such situations are not simple. In absence of any such analyses, one may simply state that the flows somehow adjust themselves in such an "ideal way" that only tangential

31

discontinuities, as assumed above, occur and the pressure equations (11) and (12) are to be satisfied. Whether such an "ideal flow" will ever be realized, particularly in case of a constant area ejector, is an open question.

Assuming that equations (11) and (12) are applicable, we now have 8 equations for the 12 unknowns involved. Another four relations are still needed to set up a determinate mathematical problem.

Homentropic Generation of the Primary and Secondary Flows

To proceed we shall now assume that the primary and secondary flows are generated homentropically (at constant entropy) from some given local stagnation (or reservoir) conditions which are assumed to take into account details of the upstream conditions leading to the primary and secondary flows as they appear at the inlet section. We denote these stagnation conditions as shown in the following table.

Stagnation Property	Flow	
	Primary	Secondary
pressure	p_{t_0}	p_{t_1}
density	ρ_{t_0}	ρ_{t_1}
enthalpy	H_0	H_1
entropy	s_0	s_1
temperature	T_{t_0}	T_{t_1}

Now, according to the relations of homentropic flow we have

32

$$h_0 + \frac{u_0^2}{2} = H_0 \qquad (13)$$

$$S_0 = s_0 \qquad (14)$$

and,

$$h_1 + \frac{u_1^2}{2} = H_1 \qquad (15)$$

$$S_1 = s_1 \qquad (16)$$

Remarks

With the use of equations (8) and (9), equations (1) through (6), (11), (12), and (13) through (16) form a system of twelve equations for the twelve unknowns enumerated before, namely ρ_0, p_0, h_0, u_0; ρ_1, p_1, h_1, u_1; and ρ_2, p_2, h_2, u_2. Admissible solutions of these equations are determined according to the entropy condition (7). We have thus formulated a determinate mathematical problem for the ejector flow under consideration.

5.3 OUTLINE OF METHOD OF SOLUTION

We note that equations 4, 5, 11, 13, 14, 15, and 16 (where in 14 and 16, S_0 and S_1 have already been expressed, by means of 8 and 9, in terms of (p_0, ρ_0) and (p_1, ρ_1), respectively) relate the eight unknowns ρ_0, p_0, h_0, u_0, ρ_1, p_1, h_1, u_1 to one another. We may, therefore, express any seven of these in terms of the remaining unknown. It is convenient to choose h_0 as this primary unknown and express

$$p_0 = p_0(h_0), \quad \rho_0 = \rho_0(h_0), \quad u_0 = u_0(h_0) \qquad (17)$$

$$h_1 = h_1(h_0) \qquad (18)$$

$$p_1 = p_0 = p_0(h_0), \quad \rho_1 = \rho_1(h_0), \quad u_1 = u_1(h_0) \qquad (19)$$

With the use of these relations, equations 1, 2, 3, 6 and 12 form a system of five equations for the five unknowns h_0, ρ_2, p_2, h_2, and u_2.

33

In order to proceed with the simultaneous solutions of the equations it is convenient to introduce a fictitious "inlet flow" (entering the ejector inlet section) and define the following fictitious quantities: density ρ_i, pressure p_i, enthalpy h_i, entropy s_i, and velocity u_i, by means of the following equations:

$$\rho_i u_i = \frac{A_0}{A_2} \rho_0 u_0 + \frac{A_1}{A_2} \rho_1 u_1 \tag{20}$$

$$P_i = \frac{A_0}{A_2} p_0 + \frac{A_1}{A_2} p_1 \tag{21}$$

$$\rho_i u_i^2 = \frac{A_0}{A_2} \rho_0 u_0^2 + \frac{A_1}{A_2} \rho_1 u_1^2 \tag{22}$$

$$\rho_i(h_i + \frac{u_i^2}{2})u_i = \frac{A_0}{A_2}\rho_0(h_0 + \frac{u_0^2}{2})u_0 \tag{23}$$
$$+ \frac{A_1}{A_2}\rho_1(h_1 + \frac{u_1^2}{2})u_1$$

$$\rho_i s_i u_i = \frac{A_0}{A_2}\rho_0 s_0 u_0 + \frac{A_1}{A_2}\rho_1 s_1 u_1 \tag{24}$$

We further introduce the following notation

$$\rho_i u_i \equiv m_i \tag{25}$$

$$P_i + \rho_i u_i^2 \equiv I_i \tag{26}$$

$$h_i + \frac{u_i^2}{2} \equiv H_i \tag{27}$$

and note that, in light of the relations 17, to 19, m_i, I_i and H_i are functions of h_0 only and are positive

$$m_i = m_i(h_0) > 0$$

$$I_i = I_i(h_0) > 0$$

$$H_i = H_i(h_0) > 0$$

Consider next the equation (6). We have, using Equation

34

(12)

$$h_2 = h_2(p_2, \rho_2)$$

$$= h_2(p_2 = p_a, \rho_2)$$

$$= h_2(\rho_2) \text{ only} \tag{28}$$

since p_a is specified.

With the use of the above definitions and relations and the Equation 6, equations 1 to 3 take following form

$$\rho_2 u_2 = \rho_i u_i = m_i(h_\emptyset) > 0 \tag{29}$$

$$p_a + \rho_2 u_2^2 = p_i + \rho_i u_i^2 = I_i(h_\emptyset) > 0 \tag{30}$$

$$2 u_2 [h_2(\rho_2) + \frac{u_2^2}{2}] = \rho_i u_i (h_i + \frac{u_i^2}{2})$$

$$\tag{31}$$

$$= m_i H_i > 0$$

or,

$$h_2(\rho_2) + \frac{u_2^2}{2} = h_i + \frac{u_i^2}{2} = H_i(h_\emptyset) > 0$$

These are three equations for the three unknowns involved namely $h_\emptyset$, ρ_2 and u_2. *Admissible solutions* of these equations (solved simultaneously) are those that fulfill the entropy condition 7. Utilizing equations 10 and 12 we have

$$S_2 = S_2(p_2, \rho_2)$$

$$= S_2 (p_2 = p_a, \rho_2) \tag{32}$$

$$= S_2(\rho_2) \text{ only}$$

since p_a is specified. Consequently, the entropy condition now takes the form

$$\rho_2 S_2(\rho_2) u_2 - \rho_i u_i S_i = \rho_2 S_2(\rho_2) u_2 - m_i(h_\emptyset) S_i(h_\emptyset) > 0$$

or, simply the form $\tag{33}$

$$S_2(\rho_2) - S_i(h_\emptyset) > 0$$

It is interesting to observe that the equations 29 to 31,

35

and 33 are similar to those for a stationary normal or shock discontinuity, as may be expected. It is, however, important to bear in mind that, since the relations between ρ_i, p_i and h_i pertaining to the fictitious inlet flow are not of the same form as for a simple fluid (as evidenced by the equations 20 to 24), the solutions for the present ejector flow should be expected to be different from those for the normal discontinuity.

5.4 SOLUTION FOR A PERFECT GAS WITH CONSTANT SPECIFIC HEATS

We shall apply our considerations to an ejector flow where the fluids constituting the primary, secondary and mixed flows are all perfect gases with constant specific heats with the same gas constant R, specific heats C_p and C_v and the same entropy constants. We then have

$$p_j = \rho_j R T_j \tag{34}$$

$$h_j = C_p T_j = \frac{\gamma}{\gamma - 1} \frac{p_j}{\rho_j} \tag{35}$$

and,

$$S_j = C_v \ln \frac{p_j}{\rho_j^\gamma} + \text{const.} \tag{36}$$

where,

$$\gamma = \frac{C_p}{C_v}$$

and j may be 0, 1, or 2.

Equations 14 and 15 now take the form

$$\frac{p_0}{\rho_0^\gamma} = \frac{p_{t_0}}{\rho_{t_0}^\gamma} \tag{37}$$

36

$$\frac{p_1}{\rho_1^\gamma} = \frac{p_{t_1}}{\rho_{t_1}^\gamma} \tag{38}$$

It then follows that

$$\frac{h_\emptyset}{H_\emptyset} = \frac{T_\emptyset}{T_{t_\emptyset}} = \left(\frac{\rho_\emptyset}{\rho_{t_\emptyset}}\right)^{\gamma-1} = \left(\frac{p_\emptyset}{p_{t_\emptyset}}\right)^{\frac{\gamma-1}{\gamma}} \tag{39}$$

and,

$$\frac{h_1}{H_1} = \frac{T_1}{T_{t_1}} = \left(\frac{\rho_1}{\rho_{t_1}}\right)^{\gamma-1} = \left(\frac{p_1}{p_{t_1}}\right)^{\frac{\gamma-1}{\gamma}} \tag{40}$$

Utilizing the pressure continuity relation (11) which is

$$p_\emptyset = p_1$$

and, introducing the following notation

$$P \equiv \frac{p_{t_\emptyset}}{p_{t_1}} \tag{41}$$

$$\xi \equiv P^{\frac{\gamma-1}{\gamma}} \tag{42}$$

$$\theta \equiv \frac{T_{t_\emptyset}}{T_{t_1}} = \frac{H_\emptyset}{H_1} \tag{43}$$

We obtain from (39) and (40) the relation

$$\frac{h_1}{h_\emptyset} = \frac{T_1}{T_\emptyset} = \frac{1}{(\rho_1/\rho_\emptyset)} = \frac{\xi}{\theta} \tag{44}$$

We note that (ξ/θ) is a constant for given P, θ, γ and   .

37

Denoting by h the ratio h_0/H_0

$$h \equiv \frac{h_0}{H_0} \tag{45}$$

We conclude explicitly that

$$p_0 = p_1 = p_t{}_0 h^{\frac{\gamma}{\gamma-1}} \tag{46}$$

$$\rho_0 = \rho_t{}_0 h^{\frac{1}{\gamma-1}} \tag{47}$$

$$\rho_1 = \frac{\theta}{\xi} \rho_t{}_0 h^{\frac{1}{\gamma-1}} \tag{48}$$

$$h_1 = \frac{\xi}{\theta} H_0 h \tag{49}$$

From equations (13) and (15), utilizing (49) in (15), we obtain

$$u_0^2 = 2 H_0 (1-h)$$

and,

$$u_1^2 = \frac{1}{\theta} 2H_0 (1-\xi h)$$

Introduce the convenient notation

$$V_{m_0}^2 = 2H_0 \tag{50}$$

Where V_{m_0} represents the maximum velocity obtainable for the primary flow by homentropic expansion from the stagnation enthalpy H_0. We then have

$$u_0^2 = V_{m_0}^2 (1 - h) \tag{51}$$

$$u_1^2 = V_{m_0}^2 \frac{1}{\theta} (1-\xi h) \tag{52}$$

The functions $m_1(h_0)$, $I_1(h_0)$, and $H_1(h_0)$ can now be

established by using the relations 46 to 52 in the equations 20 to 23 and 25 to 27. For this purpose it is convenient to introduce the following non-dimensional parameters in addition to P, ξ, θ and h defined previously:

$$\underset{\sim}{A}_{\emptyset} \equiv \frac{A_{\emptyset}}{A_2} \tag{53.1}$$

$$\underset{\sim}{A}_1 \equiv \frac{A_1}{A_2} \tag{53.2}$$

$$\underset{\sim}{A}_i \equiv \underset{\sim}{A}_{\emptyset} + \underset{\sim}{A}_1 \tag{53.3}$$

$$\underset{\sim}{A}^{\star} \equiv \underset{\sim}{A}_{\emptyset} + \frac{\underset{\sim}{A}_1}{\xi} \tag{53.4}$$

$$m \equiv \frac{m_i}{\rho_{t_{\emptyset}} V_{m_{\emptyset}}} \tag{53.5}$$

$$I \equiv \frac{I_i}{\rho_{t_{\emptyset}} V_{m}^2{}_{\emptyset}} \tag{53.6}$$

$$H \equiv \frac{H_i}{H_{\emptyset}} \tag{53.7}$$

$$P_a \equiv \frac{P_a}{P_{t_{\emptyset}}} \tag{53.8}$$

$$\rho \equiv \frac{\rho_2}{\rho_{t_{\emptyset}}} \tag{53.9}$$

$$u \equiv \frac{u_2}{V_{m_{\emptyset}}} \tag{53.10}$$

$$\alpha \equiv \frac{1}{\gamma - 1} \; ; \qquad \beta \equiv \frac{\gamma + 1}{2\gamma} \qquad (53.11)$$

Note that

$$\rho_{t_\emptyset} \, V_{m_O}^2 = 2 \; \rho_{t_0} H_\emptyset \; = \frac{2\gamma}{\gamma - 1} \; p_{t_\emptyset} \qquad (53.12)$$

The following expressions in non-dimensional form are obtained:

$$m(h) = h^\alpha \, (\underset{\sim}{A}_O \, \sqrt{1-h} + \underset{\sim}{A}_1 \, \frac{\sqrt{\theta}}{\xi} \, \sqrt{1- \xi h}) \qquad (54)$$

$$I(h) = h^\alpha \, (\underset{\sim}{A}^* - \, 3\underset{\sim}{A}_i \, h) \qquad (55)$$

$$m(h) \, H(h) = h^\alpha \, (\underset{\sim}{A}_\emptyset \, \sqrt{1-h} + \underset{\sim}{A}_1 \, \frac{1}{\xi\sqrt{\theta}}\sqrt{1- \xi h}) \qquad (56)$$

Equation (28), which in light of Equation 12, expresses the equation of state for the mixed flow now takes the explicit form

$$\rho_2 h_2 = \frac{\gamma}{\gamma - 1} \; p_a \; , \quad \text{a constant} \qquad (57)$$

Now, the three basic equations (29) to (31) governing the unknowns $h_\emptyset$, ρ_2, and u_2 can be expressed in nondimensional form as

$$\rho u \; = m(h) \; > \emptyset \qquad (58)$$

$$\rho u^2 = I(h) - \frac{\gamma - 1}{2\gamma} \; P_a \; > 0 \qquad (59)$$

$$P_a u + \rho u^3 = m(h) \, H(h) \; > \emptyset \qquad (60)$$

Where, $m(h)$, $I(h)$, and $H(h)$ are given by (54) to (56).

From these equations eliminating u and introducing the notation

$$\zeta(h) = \zeta \equiv I(h) - \frac{\gamma - 1}{2\gamma} \; P_a \; > 0 \qquad (61)$$

we obtain,

$$\zeta^2 + P_a\zeta = m^2 H \tag{62}$$

where ζ, m, and H are functions of h only. Thus, this equation is an explicit single equation containing only h as the unknown. With the use of the Eqs. 54 to 56 it takes the form (where,

$$\eta = \frac{\gamma - 1}{2\gamma})$$

$$[h^\eta (A^* - A_1 h) - P_a]^2 + P_a[h^\eta (\zeta^* - \zeta_1 h) - P_a]$$

$$= h^{2\eta} (A_0 \sqrt{1-h} + A_1 \sqrt{\_} \sqrt{1-h})$$

$$(A_0 \sqrt{1-h} + A_1 \frac{1}{\sqrt{\_}} \sqrt{1-h}) \tag{63}$$

Note that $\eta = 1/(\gamma-1)$ and that $\gamma = (\gamma+1)/2\gamma$. If $\gamma = 1.4$, we have $\gamma = 2.5$, $\eta = 0.857$, $\gamma = 0.143$. In such a case the equation involves h^7 implying in general seven roots for h.

Corresponding to each root of this equation one obtains, on the basis of equations 46 to 52, a set of values for the primary and secondary flow quantities ζ, p_0, q_0 and η_1, ζ_1, p_1 and q_1 respectively and consequently for m, H and I.

The solution for ζ or equivalently I, for each root of h is readily obtained from Equation 62 as

$$\zeta = I - \gamma P_a = \sqrt{m H + \left(\frac{P_a}{2}\right)^2} - \frac{P_a}{2} \tag{64}$$

since, $\zeta > 0$.

Equations 62 and 64 give, for each root of h, to the solutions for the primary q_0 and the density ρ_0 of the mixed

flow. They are given by

$$a = \frac{l}{m} \tag{65}$$

and,

$$c = \frac{m^2}{l} \tag{66}$$

It is noteworthy to observe that the multiplicity of the solutions existing here originates with the ("poly-degree") equation for the primary unknown h_0 or equivalently h. This seems to have not been appreciated in the previous analyses of the problem presented in the literature.

Entropy Condition and Admissible Solutions

Selection of the admissible solution, out of the several roots, as discussed above, is carried out on the basis of the entropy condition (33). To proceed, we first denote by ϵ the ratio of the secondary mass flow to the primary mass flow:

$$\epsilon = \frac{A_1 \rho_1 u_1}{A_0 \rho_0 u_0} = \frac{\dot{\sigma}_1}{\dot{\sigma}_0} \qquad \frac{\sqrt{}}{?} \sqrt{\frac{1 - \tau h}{1 - h}} \tag{67}$$

where use has been made of the appropriate relations given before. We note that

$$\epsilon = \epsilon(h) \quad \text{only}$$

as expected. Then, with the basic relation (36) for entropy and other required equations and definitions previously given, one may express the entropy condition (33) in the following

-54-

nondimensional form

$$\frac{s_\emptyset - s_1}{C_v} \cdot \frac{\psi(h)}{1 + \psi(h)} + \ln \frac{P_a}{\rho^\gamma} > \emptyset \qquad (68)$$

Noting that

$$\frac{s_\emptyset - s_1}{C_v} = \gamma \ln \frac{\theta}{\xi}$$

and utilizing the solution (66) for ρ we express (68) explicitly as

$$\gamma \left[(\ln \frac{\theta}{\xi}) \frac{\psi(h)}{1 + \psi(h)} + [\ln \zeta(h) - 2\ln m(h)] + \ln P_a > \emptyset \right] \qquad (69)$$

where, $m(h)$, $\zeta(h)$ and $\psi(h)$ are given by (54), (55), (61), and (67) respectively only those roots of Equation (63) for h which fulfill this inequality (69) are the admissible solutions for h. Admissible solutions for the various properties of the primary, secondary, and mixed flows and other desired quantities such as mass and augmentation ratios are those that correspond to the admissible solutions for h. The expressions for the solutions for the flow properties are given in Table 1.

A local total enthalpy H_2 and local total temperature T_{t_2} may be defined, in the usual manner, by means of the relations

$$C_p T_{t_2} = H_2 = h_2 + \frac{u_2^2}{2}$$

From equations (31) and (62) one obtains, in nondimensional form,

43

that

$$\frac{T_{t_2}}{T_{t_\emptyset}} = \frac{H_2}{H_\emptyset} = H = \frac{\zeta^2 + P_a \zeta}{m^2}$$

Table 1. Summary of Solutions For Flow Quantities

Flow Quantity	Solution Expression For		
	Primary Flow	Secondary Flow	Mixed Flow
	$j=0$	$j=1$	$j=2$
$h_j/H_0 = T_j/T_{t_0}$	h	$\dfrac{\xi}{\theta}h$	$P_a\,\dfrac{\zeta(h)}{m^2(h)}$
$= a_j^2/a_{t_0}^2$			
p_j/p_{t_0}	$h^{\gamma/\gamma-1}$	$h^{\gamma/\gamma-1}$	P_a
ρ_j/ρ_{t_0}	$h^{1/\gamma-1}$	$h^{1/\gamma-1}$	$\dfrac{m^2(h)}{\zeta(h)}$
u_j^2/V_{m0}^2	$(1-h)$	$\dfrac{1}{\theta}(1-\xi h)$	$\dfrac{\zeta(h)}{m(h)}$
M_j^2	$\dfrac{2}{\gamma-1}(\dfrac{1}{h}-1)$	$\dfrac{2}{\gamma-1}(\dfrac{1}{\xi h}-1)$	$\dfrac{2}{\gamma-1}\dfrac{\zeta(m)}{P_a}$

Note: a_j: denotes local speed of sound

   M_j: Mach number

45

6. CONCLUSIONS AND RECOMMENDATIONS

From the experimental investigation, the following conclusions can be drawn.

Presence of ejector shroud reduced the jet spreading. Duct width over the range tested (W/D = 15 ~ 25 or area ratio = 21 ~ 35), had negligible influence on jet spreading; and on the jet center line velocoity/temperature decay.

Primary jet heating, over the temperature range tested, had no significant effect on the velocity field within the ejector or that of the free jet.

The centerline temperature decay within the ejector displayed no significant differences in comparison to the free jet, up to the location where the primary jet spreads to the mixing duct wall. Downstream of that location the center line temperature within the ejector is higher than that of the free jet. This increase is due to the fact that the center line velocity in this region decays much slower.

The present investigation, as described, furnishes some detailed experimental data which, on one hand, support some of the previous observations made on free rectangular jets, while, on the other hand, gave an account of some of the effects of duct walls on the development of the jet. These studies are not complete enough to enable a detailed understanding of the complex flow development of the jet inside the duct. All the implications of the results obtained are not yet fully understood. Further detailed investigations are clearly needed to clarify the importance of the nozzle exit temperature on the

46

flow structure. The range of parameters needs to be extended to high nozzle exit temperatures and Mach numbers.

A theoretical analysis is made to set up a determinate mathematical problem for the flow through a constant-area ejector, in terms of parameters characterizing the generation of the primary flow, the initial conditions from which the secondary flow is induced and the conditions of the ambient medium. Multiple solutions (more than two) occur, and admissible ones are those that fulfill the entropy condition.

References

1. Quinn, B., "Thrust augmenting ejectors: a review of the application of jet mechanics to V/STOL aircraft propulsion", AGARD CPP308, 1981.

2. Porter, J.J., Squyers, R.A., and Esparza, S.F., "An overview of ejector theory", AIAA Paper No. 81-1678, 1981.

3. Bevilaqua, M.R., "Evaluation of hyper mixing for thrust augmenting ejectors", Journal of Aircraft, 11. No. 6, 1974.

4. Krothapalli, A., Baganoff, D. and Karamcheti, K., "An experimental study of multiple jet mixing", Joint Institute for Aeronautics and Acoustics TR-23, Stanford University, 1979.

5. Viets, H., "Unsteady Ejectors", AGARD CPP308, 1981.

6. Bowers, L.D., "Aerodynamic effects induced by a vectored high aspect ratio non axisymmetric exhaust nozzle", Journal of Aircraft, 13, No. 12, 1976.

7. Bernal, P.L., and Sarohia, V., "Entrainment and mixing in thrust augmentaing ejectors", AIAA Paper No. 83-0172, 1983.

8. Schetz, A.J., "Injection and mixing in turbulent flow", Progress in Astronautics and Aeronautics, Vol. 68, 1980.

9. Higgins, C.C., Kelly, D.P., and Wainwright, T.W., "Tests in and out of ground effect with 70°F and 1200°F nozzle discharge temperatures", NASA CR-373, 1966.

10. Sfeir, A.A., "The velocity and temperature fields of rectangualr jets", Int. J. of Heat and Mass Transfer, 19, 1976.

11. Sforza, P.M., and Stasi, W., "Heated three-dimensional turbulent jets", ASME Paper 77-WA HT - 17, 1977.

12. Bobba, R.J., and Ghia, N.K., "A study of three-dimensional

turbulent jets", Proceedings of 2nd symposium on turbulent shear flows, 1979.

13.   Quinn, B., "Ejector performance at high tempertures and pressures", Journal of Aircraft, 13, No. 12, 1976.

14.   Hsia, Y., Krothapalli, A., Baganoff, D., and Karamcheti, K., "The structure of a subsonic compressible rectangular jet", Joint Institute for Aeromautics and Acoustics TR-43, 1982.

15. Bradbury, L.J.S., and Riley, J., "The spread of a turbulent plane jet issuing into a parallel moving stream", Journal of Fluid Mechanics, 27, part 2, 1967.

16.   Marsters, G.F., "The effects of upstream nozzle shaping on in compressible turbulent flows from rectangular nozzles", Trans. CSME, 5, No. 4 1978 - 1979.

17.   Marsters, G.F., "Spanwise velocity distributions in jets from rectangular slots", AIAA Journal, 19, No. 2, 1981.
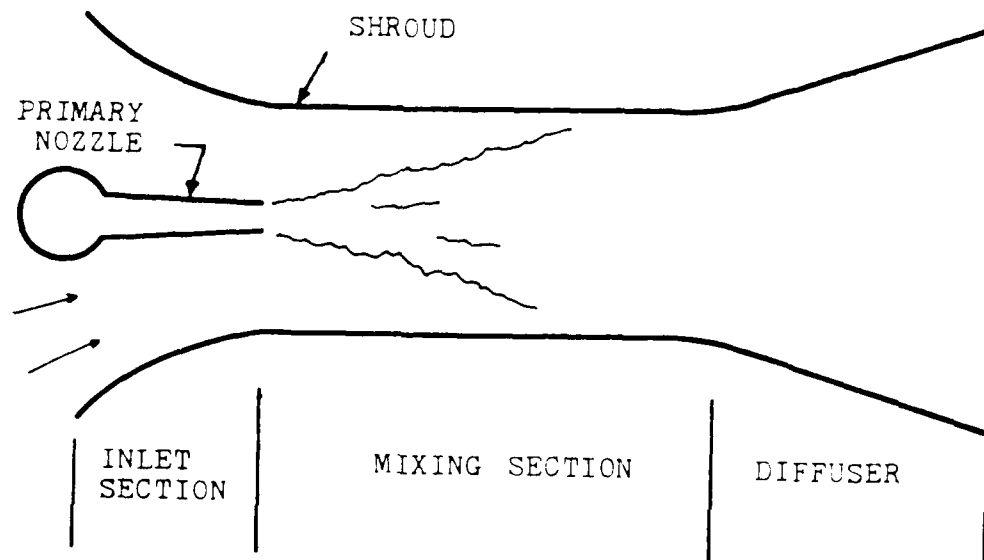
Figure 1. Schematic of an ejector

Fig. la Ejector flow under consideration

L = **50mm**
D = **5 mm**
ASPECT RATIO, L/D = 10
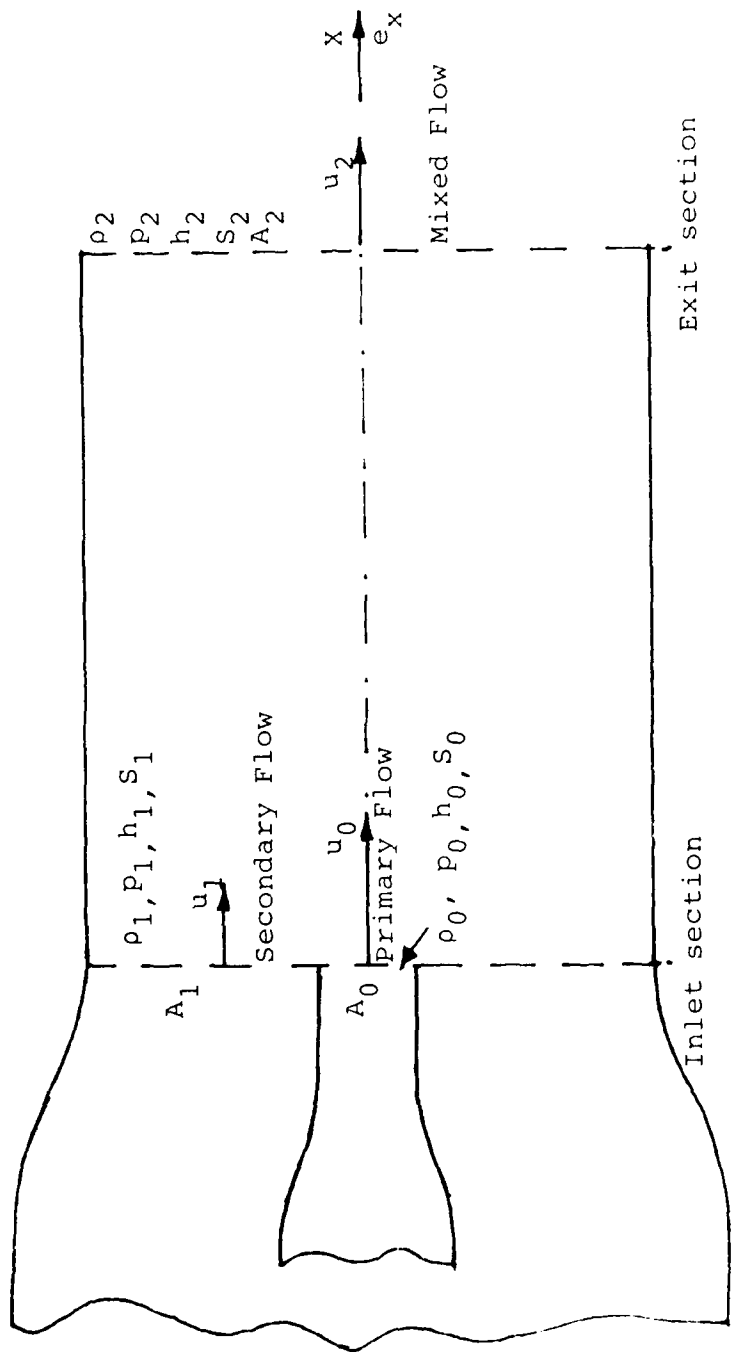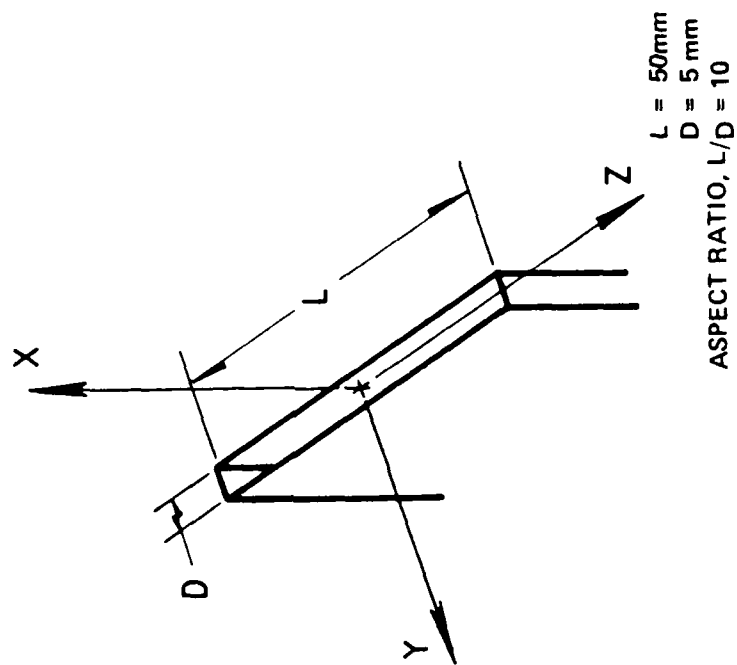
Figure 2a. Primary jet nozzle, and definitions.

52
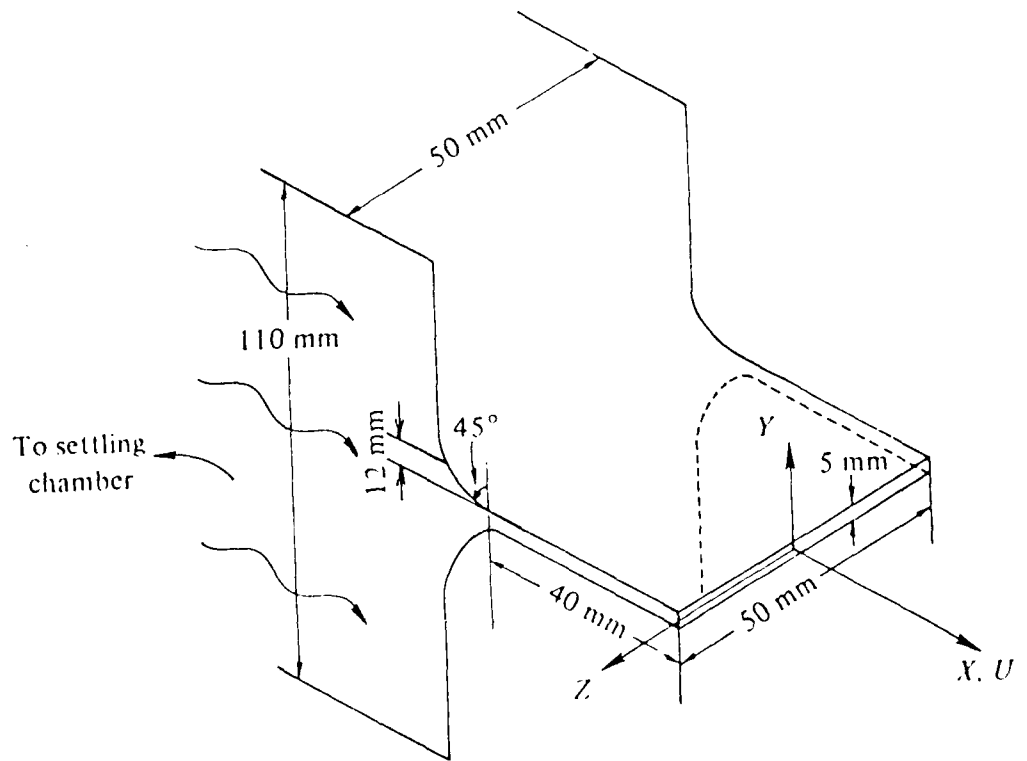
Figure 2b. Schematic of the primary nozzle
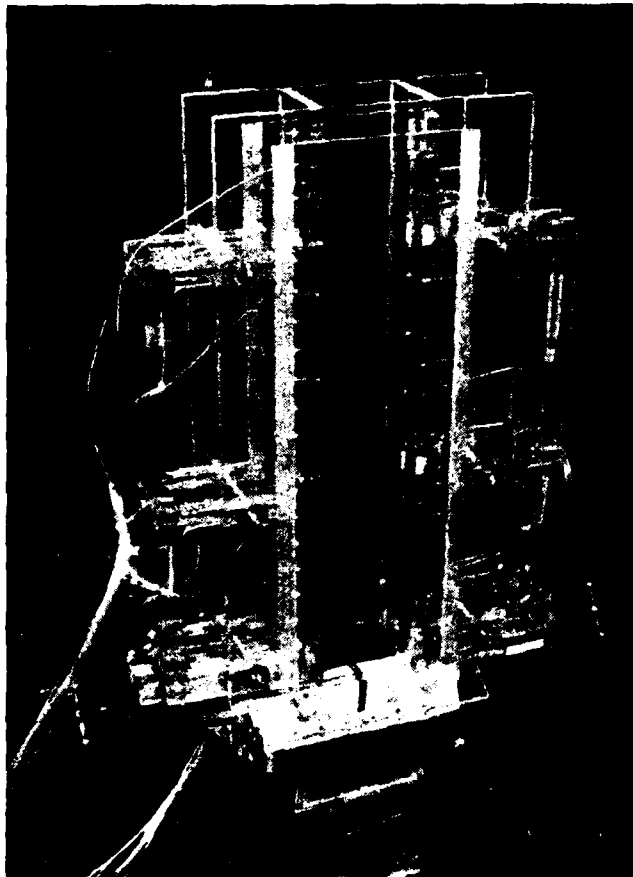
Figure 3. Ejector model.
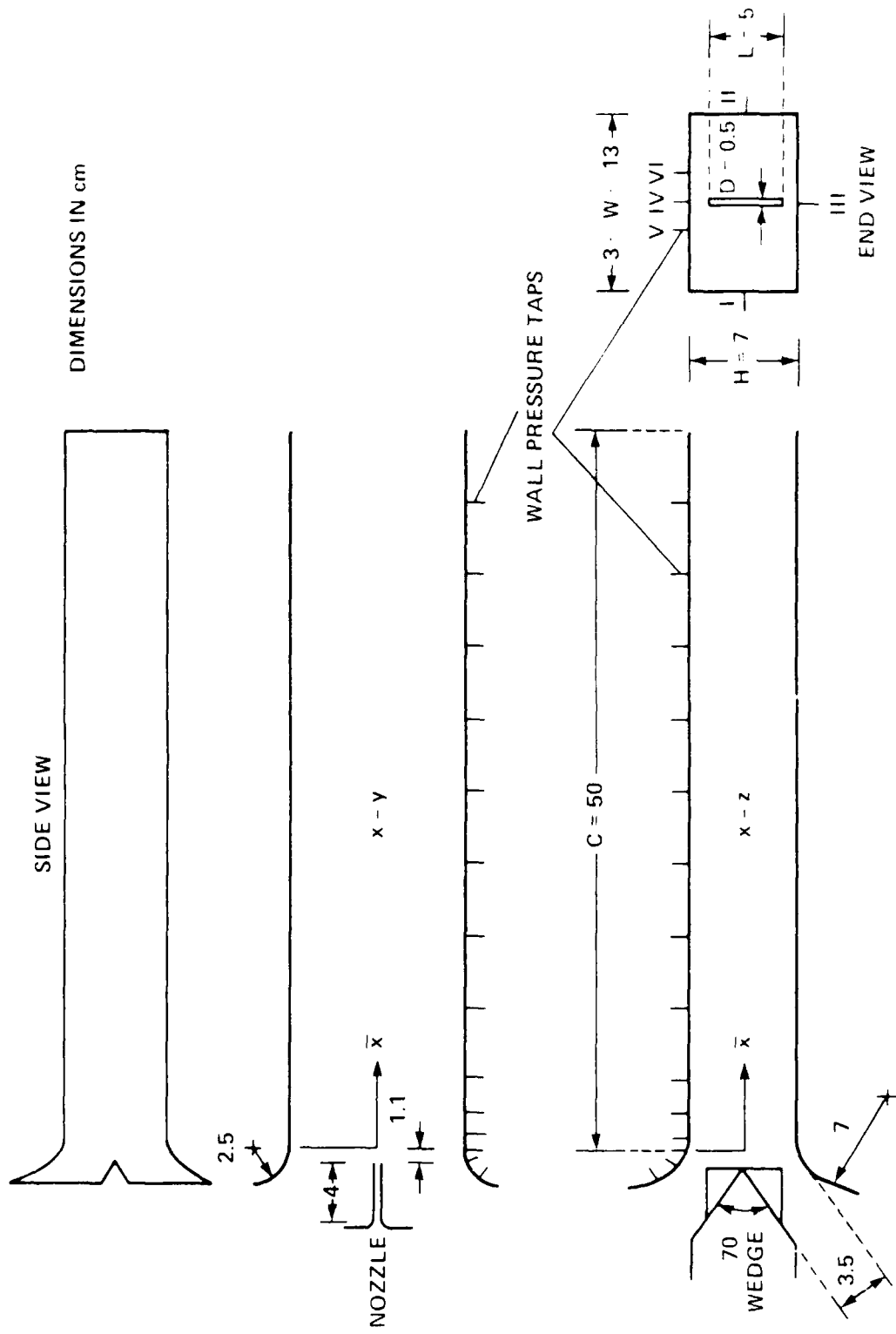
Figure 4. Schematic of the ejector model, and locations of the pressure taps.

55
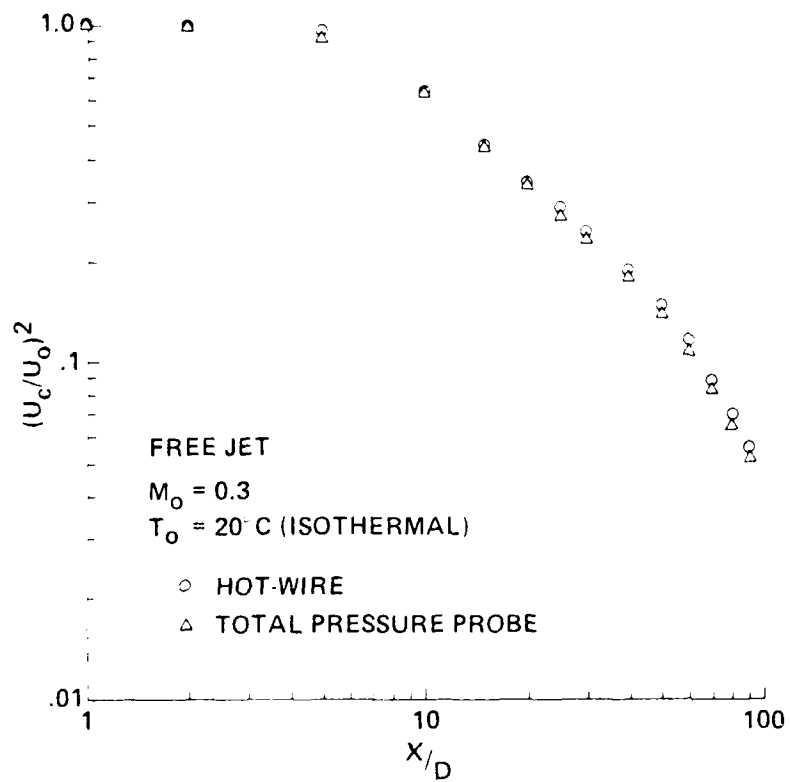
Figure 5a. A comparison of the centerline velocity decay
obtained using pitot tube and hot-wire.
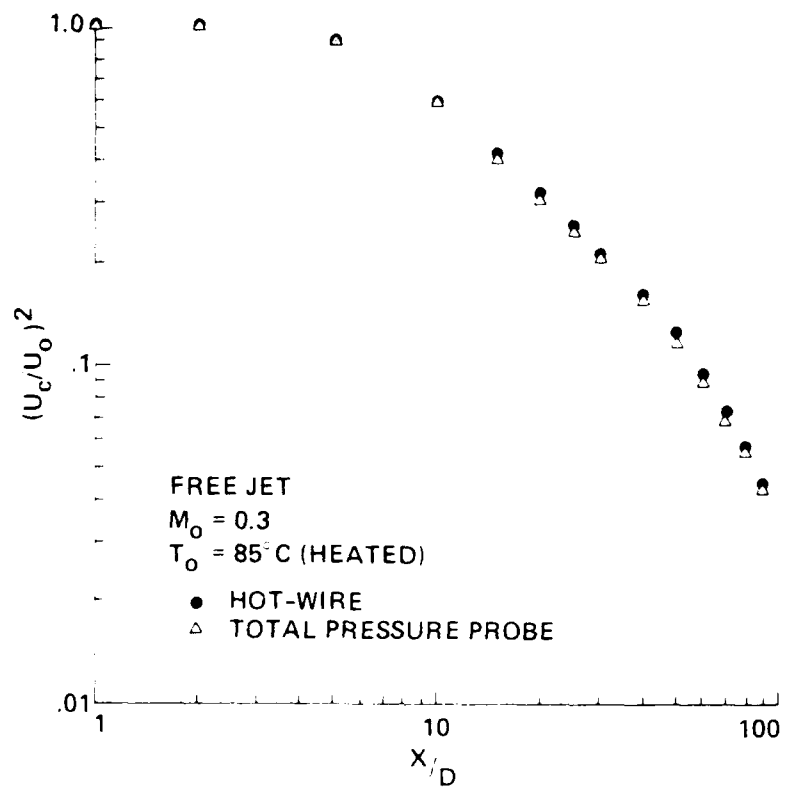
Figure 5b. A comparison of the centerline velocity decay of a heated jet obtained using pitot probe and hot-wire.

CONFINED, W/D = 20

$T_o = 75° C$

$M_o = 0.3$
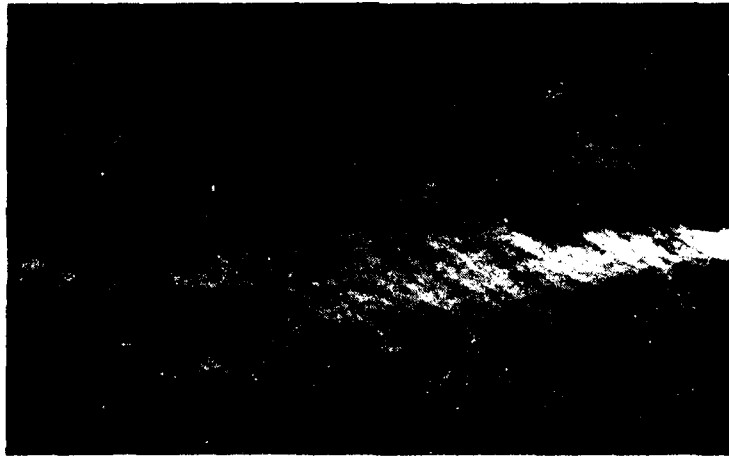
FREE

Figure 66. Schlieren photographs of the jet in the x, y plane; free jet and confined jet.

$M_o = 0.3$ $W/D = 24$
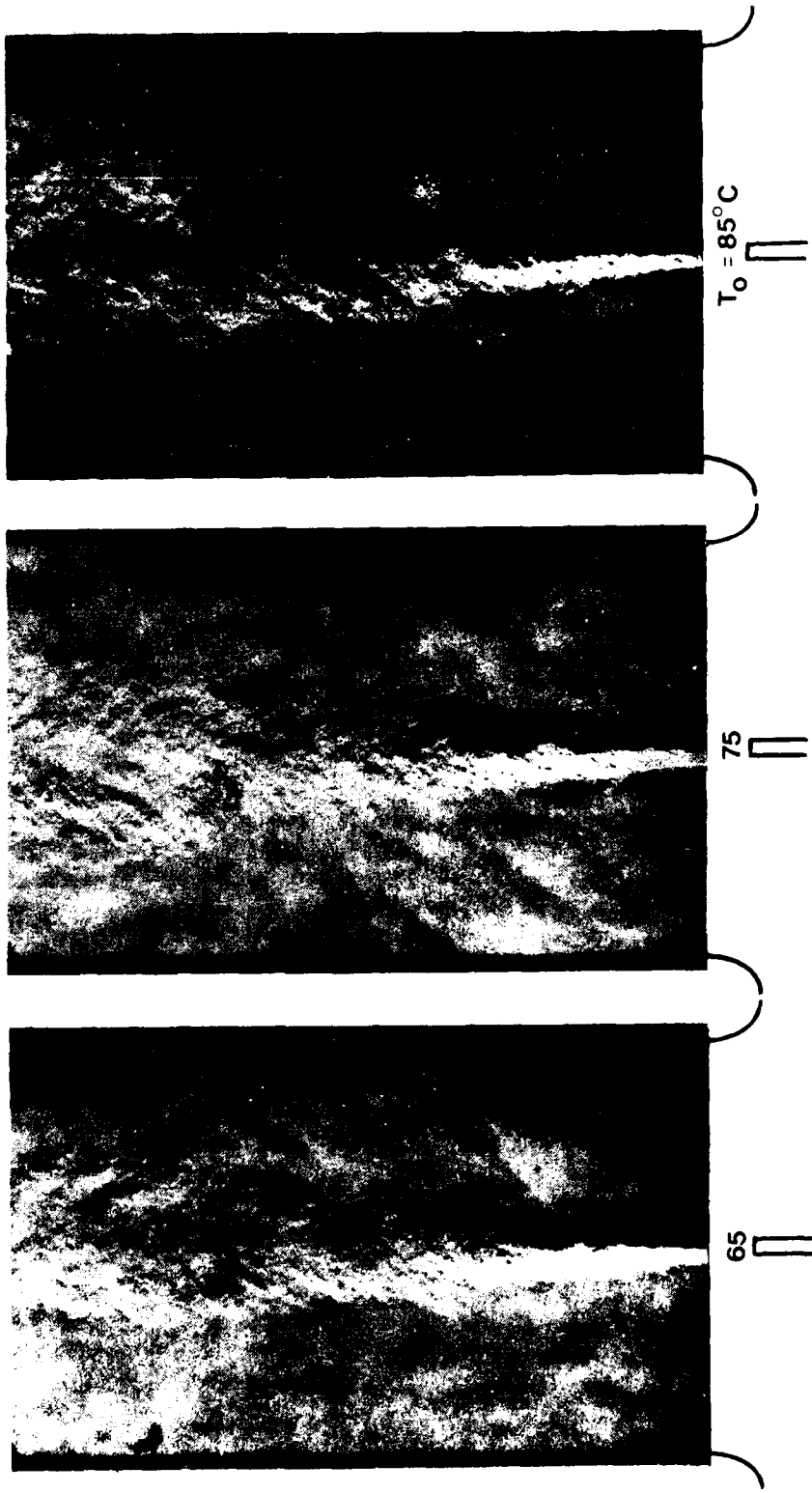
Figure 6b. Schlieren photographs of the confined jet at three different exit temperatures

59

W/D = 24   20   16

$M_o = 0.3$ $T_o = 85°C$
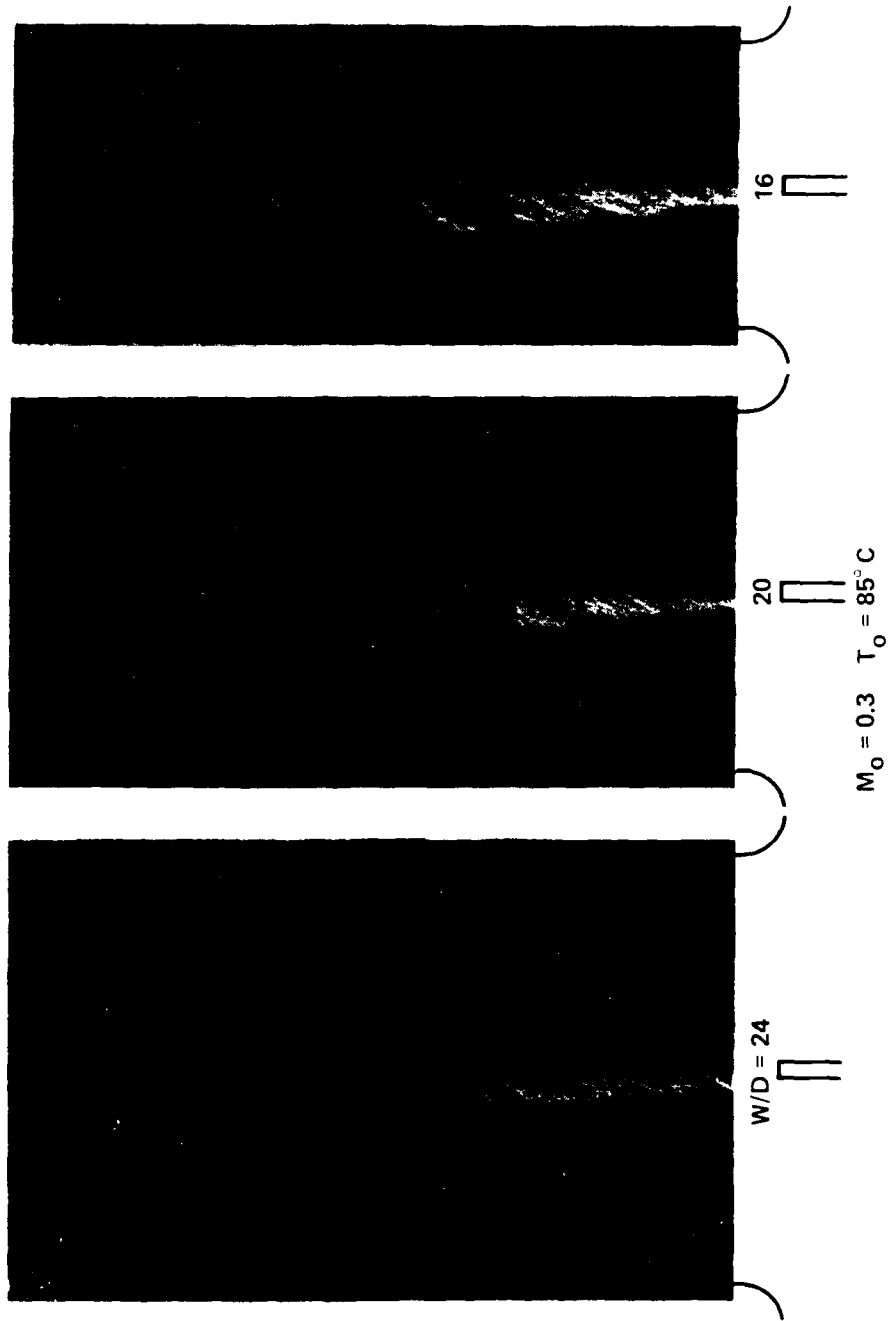
Figure 6c. Schlieren photographs of the confined jet at three different area ratios
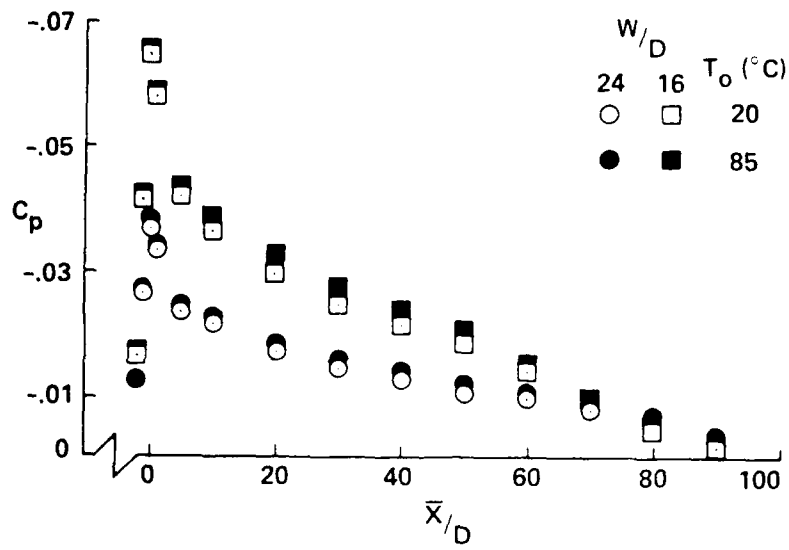
Figure 7. Effect of primary jet heating and duct width on ejector shroud surface pressure distribution.

61
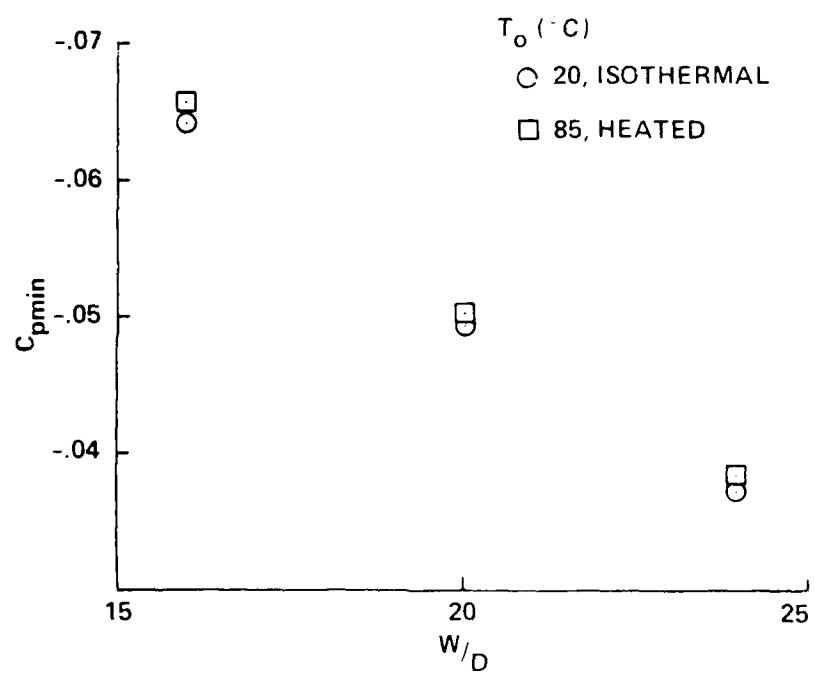
Figure 8. The variation of the throat pressure with area ratio.
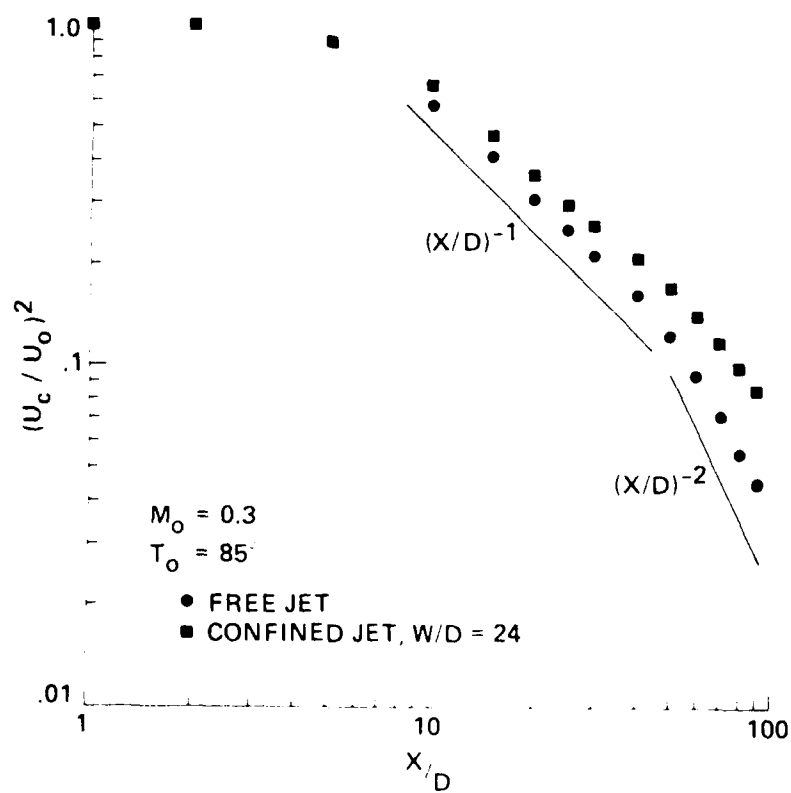
Figure 9. The effect of confinement on the centerline velocity decay.
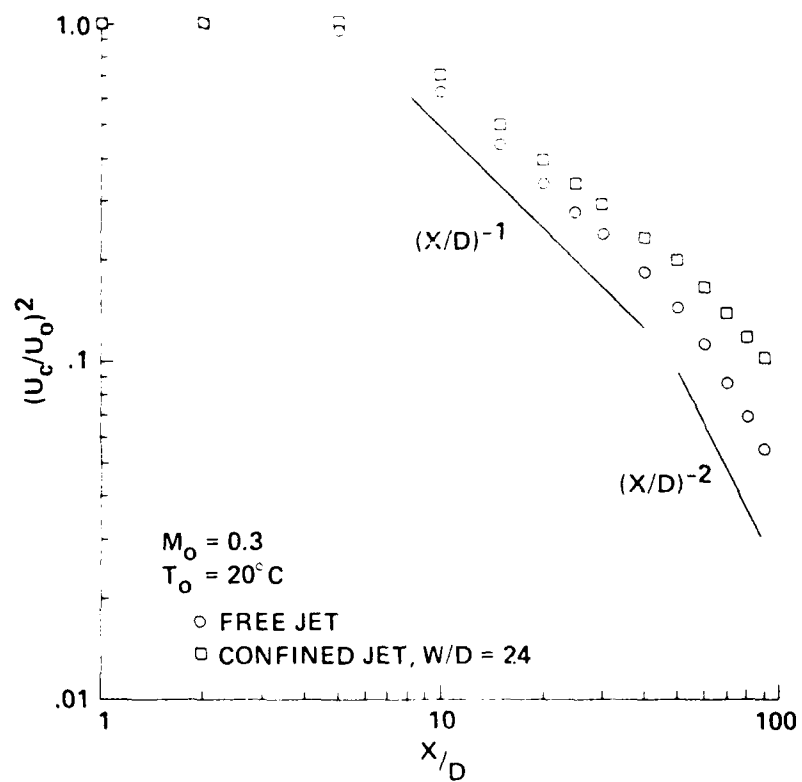
Figure 10. The effect of confinement on the center line velocity decay of an isothermal jet.
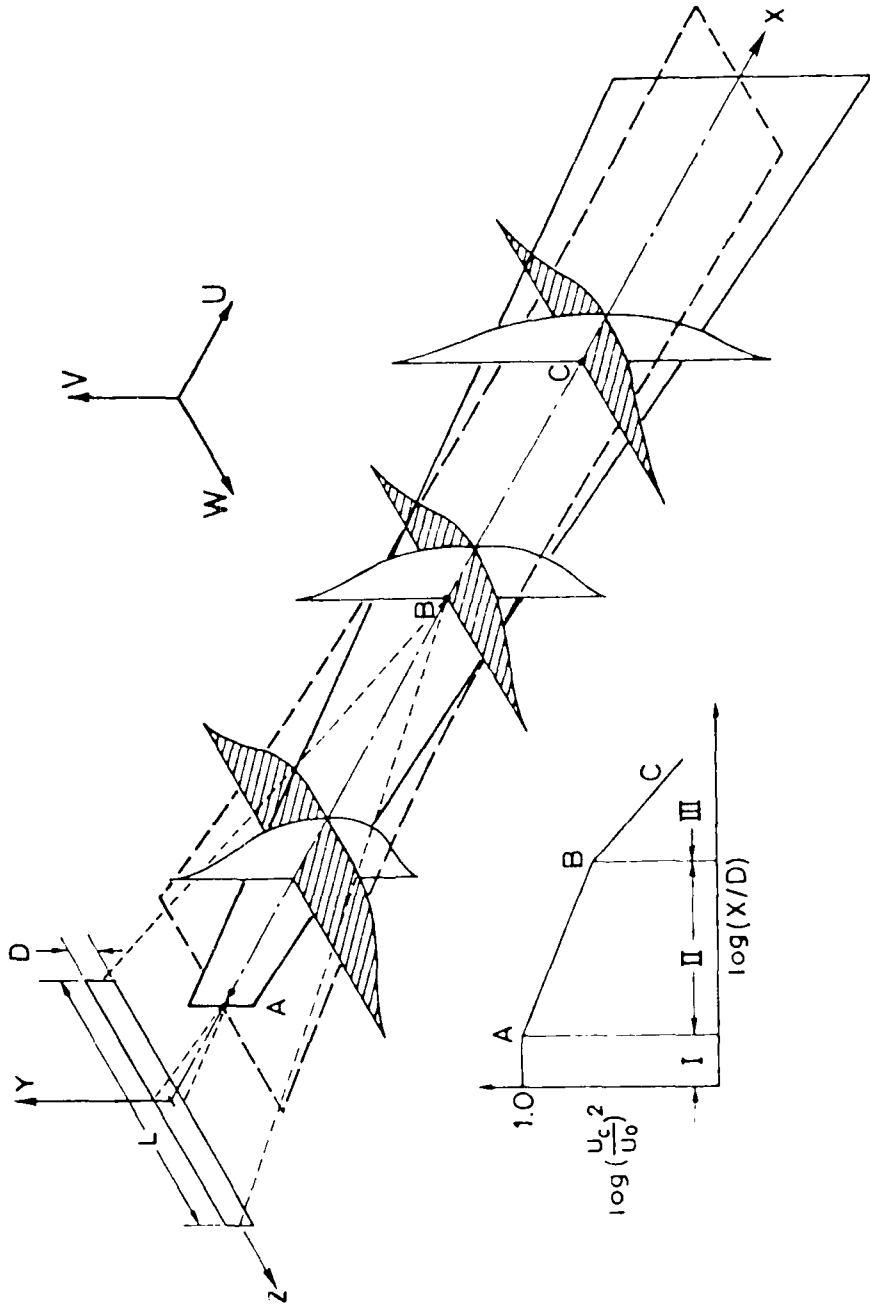
Figure 11. Schematic representation of the flow field of a rectangular free jet.
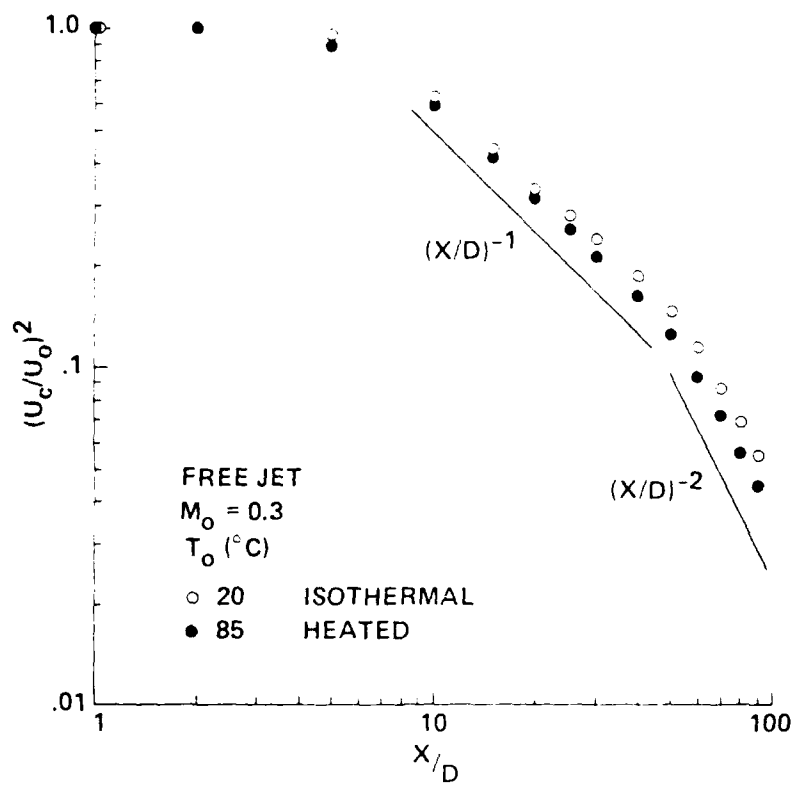
Figure 12. The decay of the mean velocity along the center line of a free jet.
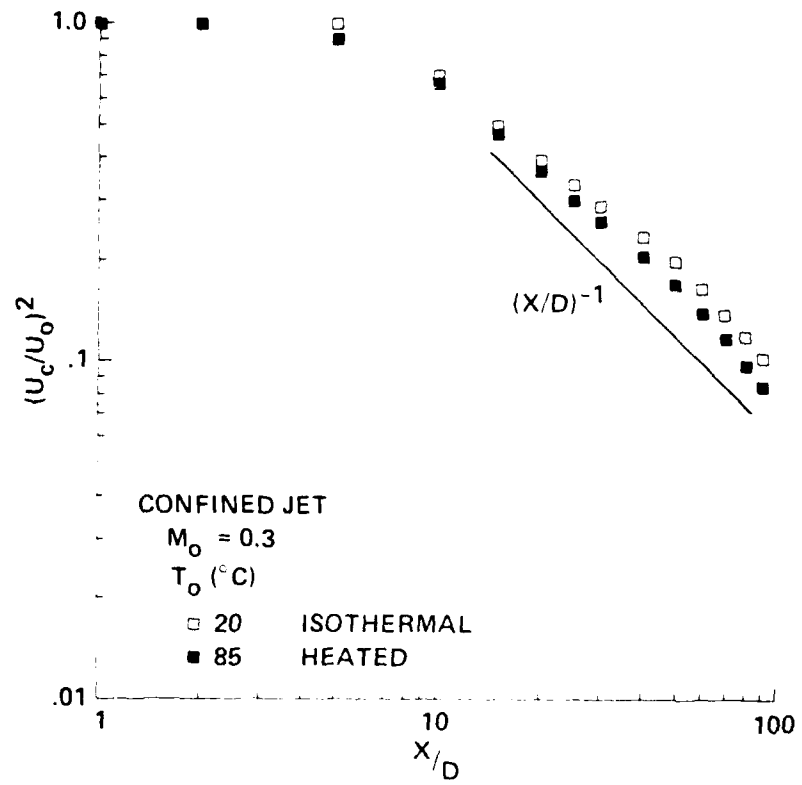
Figure 13. The decay of the mean velocity along the center line of a confined jet.
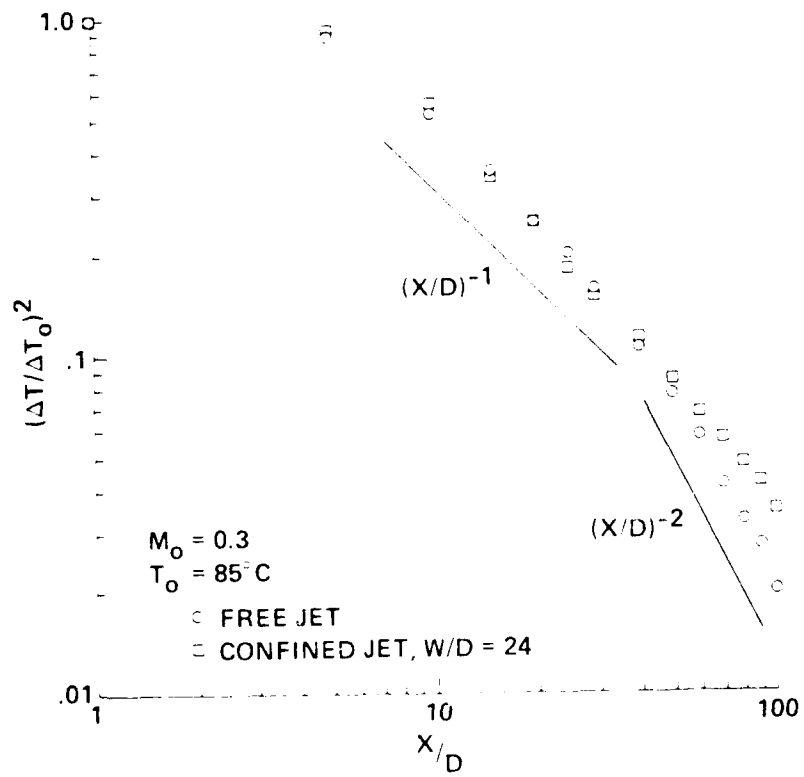
Figure 14. The decay of the total temperature along the center line of both free and confined jet.
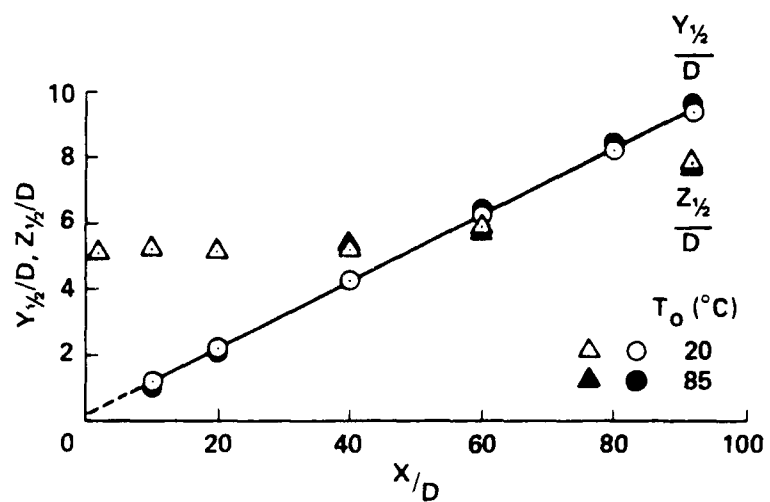
Figure 15.   Velocity half widths in the central planes of a free jet.
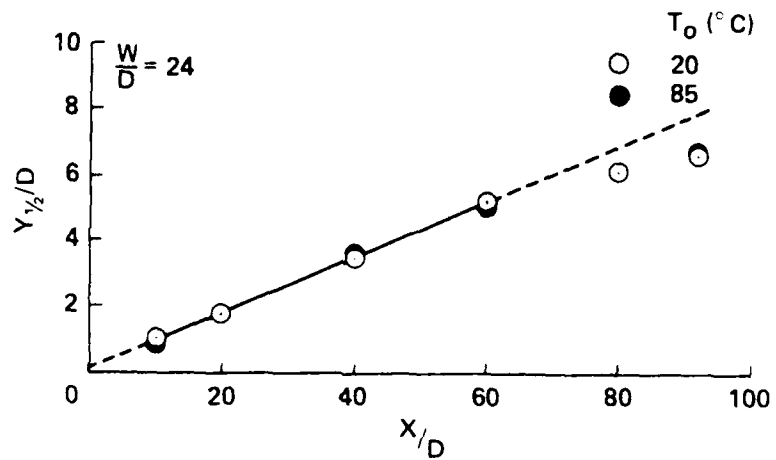
Figure 16. Velocity half widths in the central X,Y plane of a
confined jet.
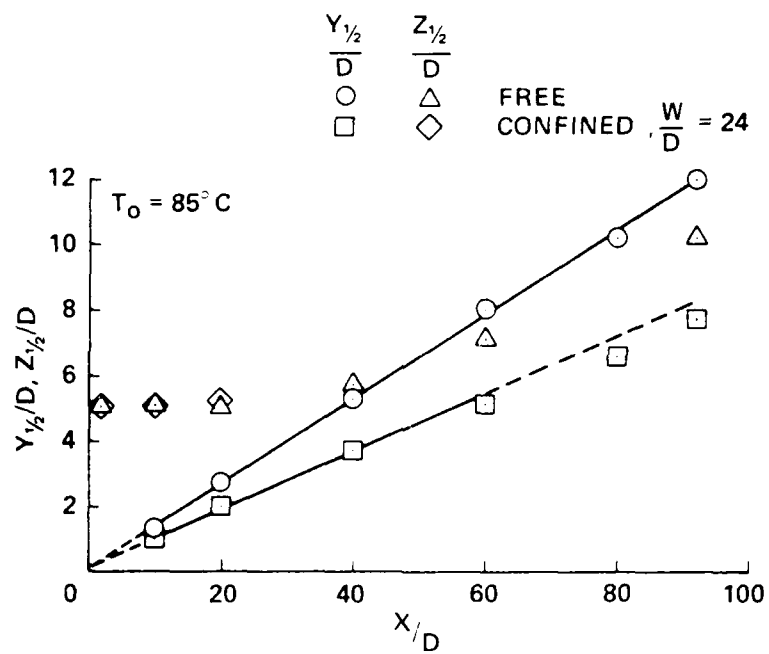
Figure 17. Temperature half widths in the central X,Y and X,Z planes of free and confined jets.

X/D = 92

80

60

40

20

10

2

10 m/s

2D

X - Y

X - Z

CONFINED JET   VELOCITY PROFILES
$M_O = 0.3$
$T_O = 20$ C
$\frac{W}{D} = 24$ $\frac{H}{D} = 14$
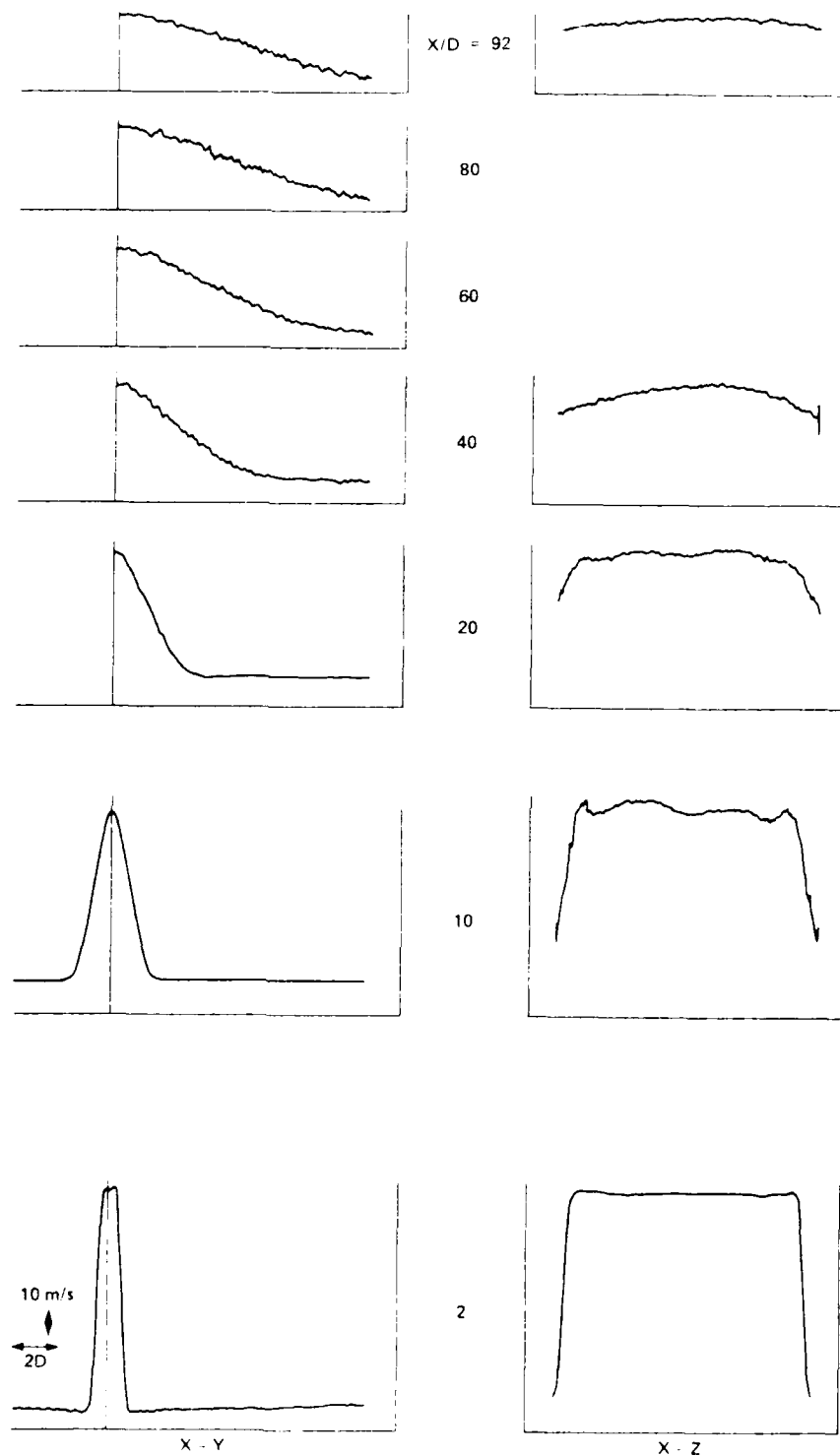
Figure 18. Mean velocity profiles in the central X,Y and X,Z planes of an isothermal confined jet.

72

X/D = 92

80

60

40

20

10

2

10m/s

2D

X - Y

X - Z

FREE JET VELOCITY PROFILES

$M_o = 0.3$
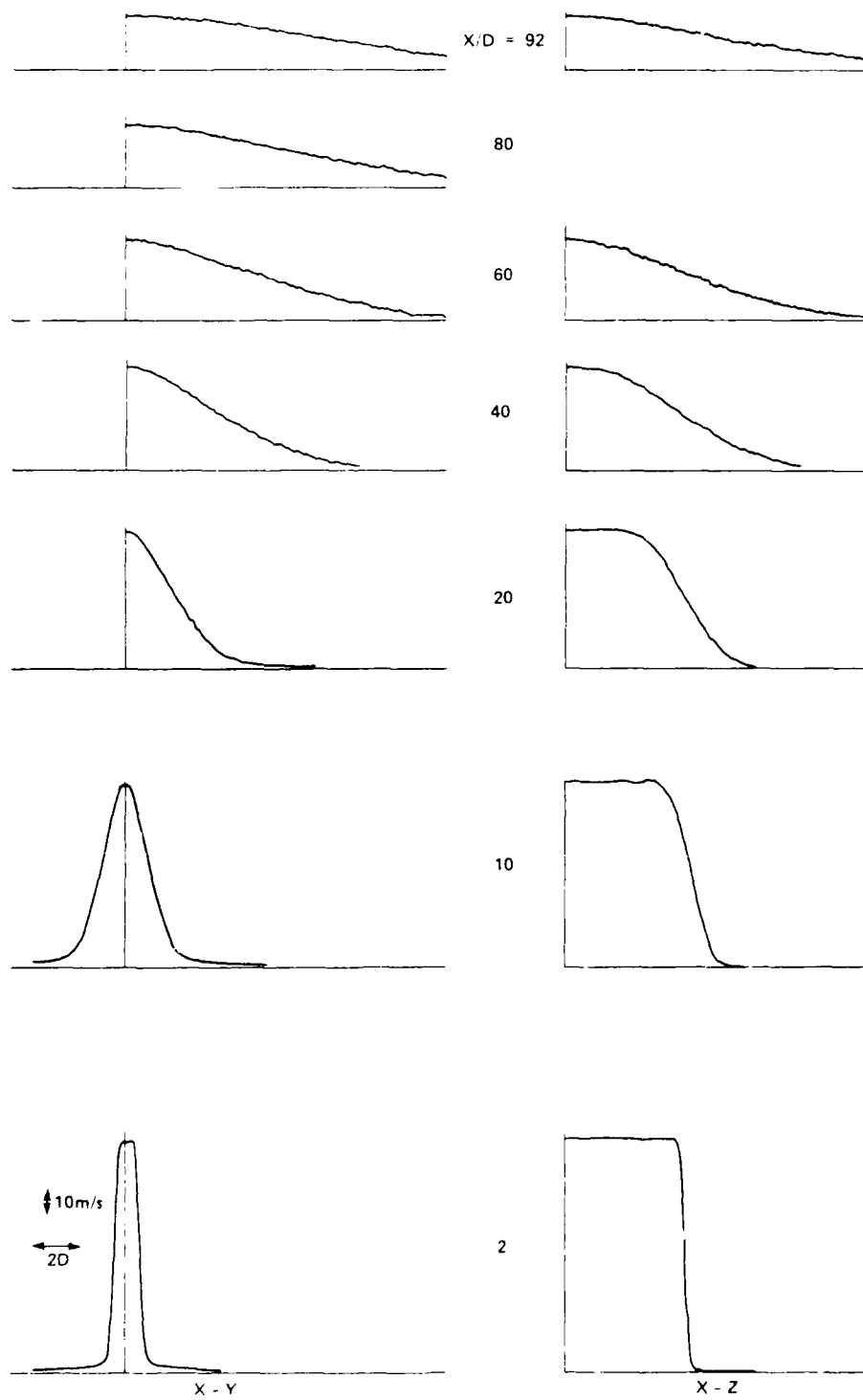
$T_o = 20$ C

Figure 19. Mean velocity profiles in the central X,Y and X,Z planes of an isothermal free jet.

73

Figure 20. Mean (time constant= 1sec) temperature profiles in the central
X,Y and X,Z planes of a confined jet.

74
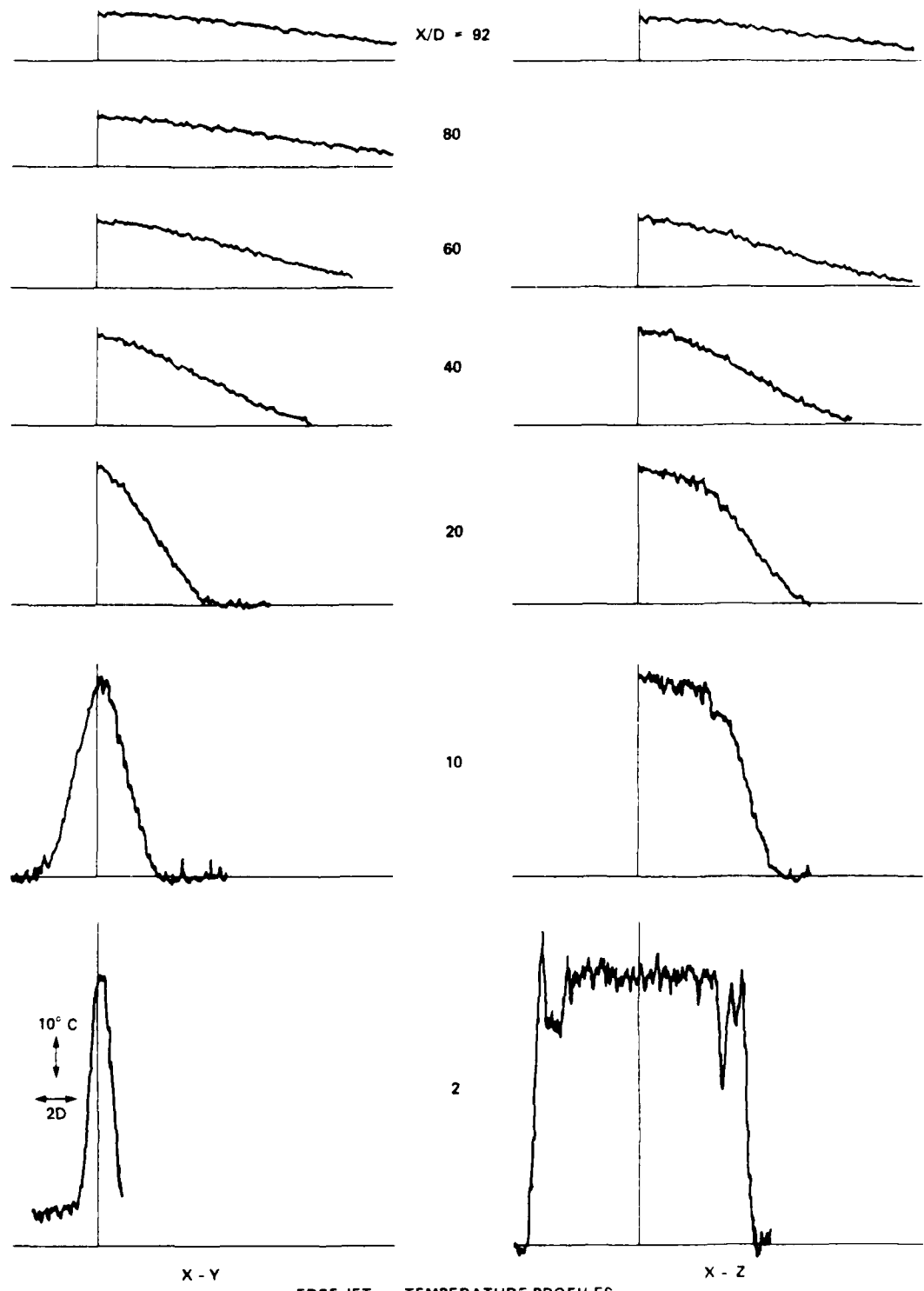
Figure 21. Mean (time constant= lsec) temperature profiles in the central
X,Y and X,Z planes of a free jet.

75
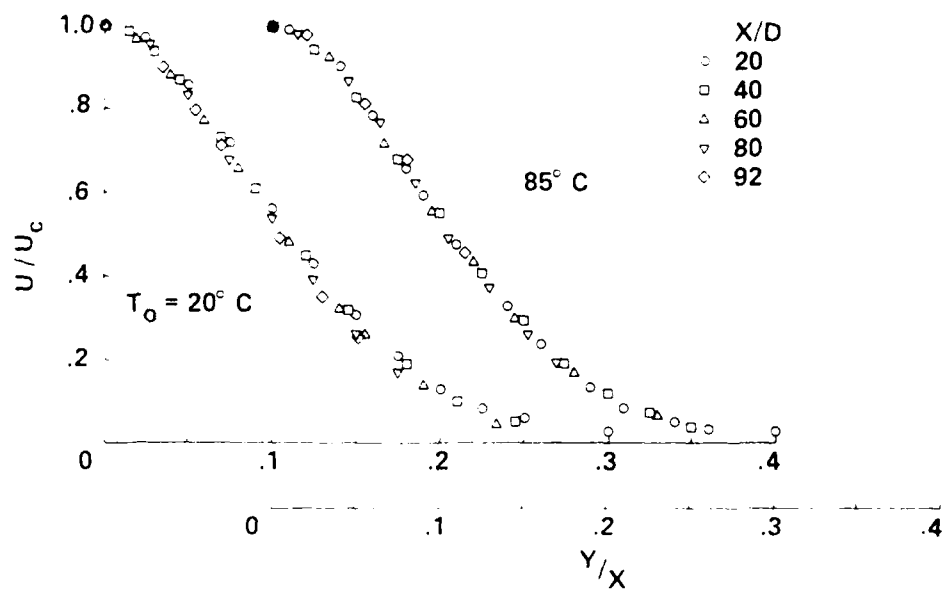
Figure 22. Mean velocity profiles in the central X,Y plane of a free jet.
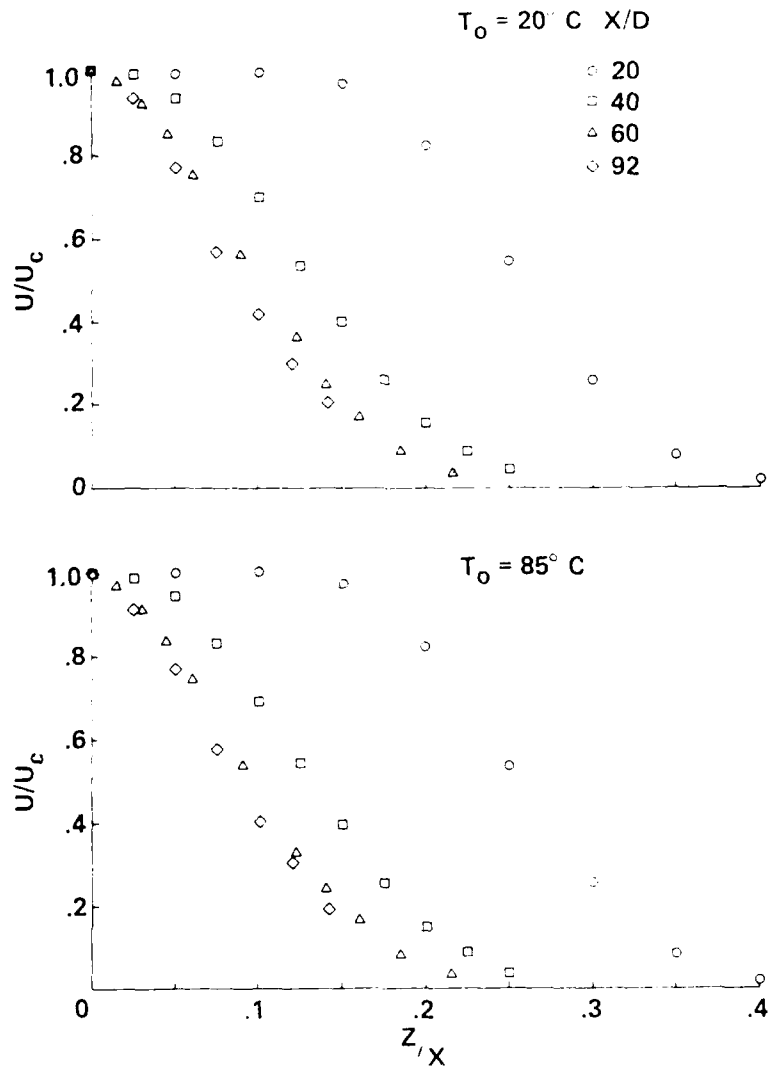
Figure 23. Mean velocity profiles in the central X,Z plane of a free jet.
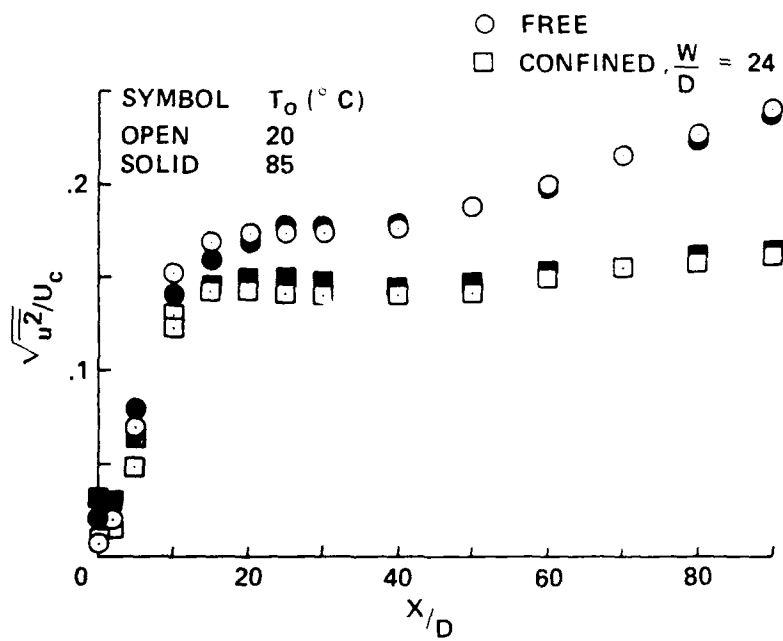
Figure 24. Variation of the turbulent intensity along the center line of free and confined jets.
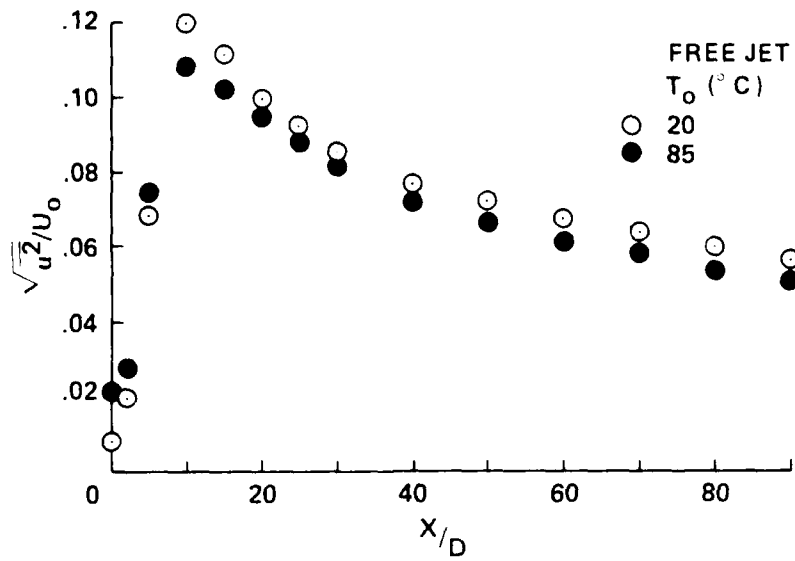
Figure 25. Variation of the turbulent intensity along the center line of the free jet.
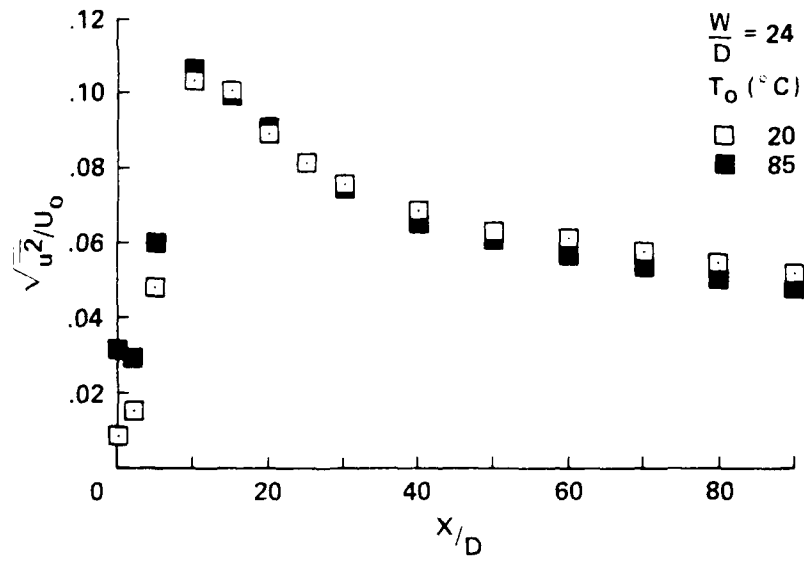
Figure 26. Variation of the turbulent intensity along the center line of the confined jet.

Appendix A

Ejector shroud surface pressure distributions at different conditions tested. (See Fig 4)

W: Duct width

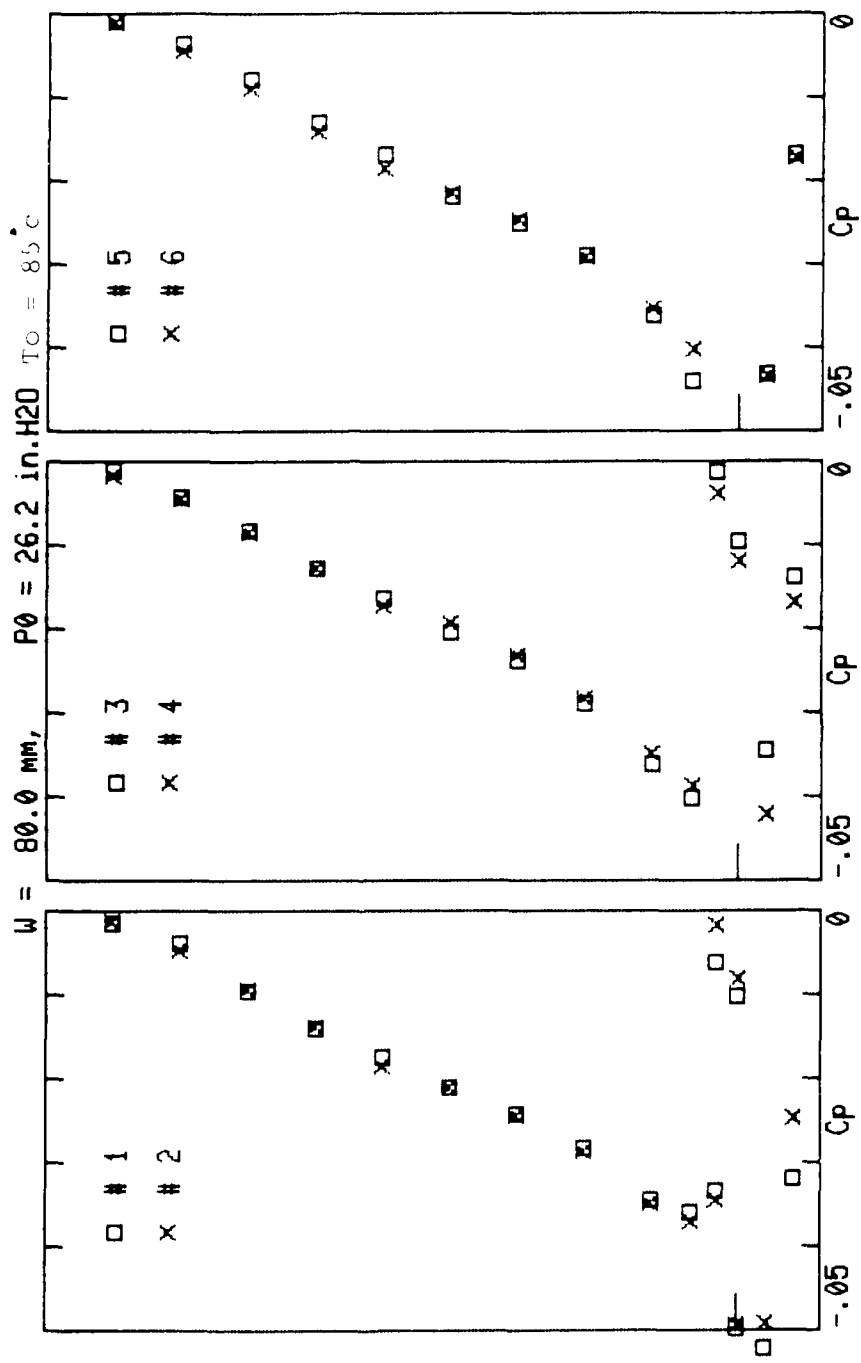$P_\emptyset$:   Primary jet plenum pressure   (M = 0.3)

$T_\emptyset$:   Nozzle exit temperature

NOTE: The pressure Taps are symmetrically located. Taps 4,5,6 are 1 cm apart. The vertical axis denotes distances along the duct.
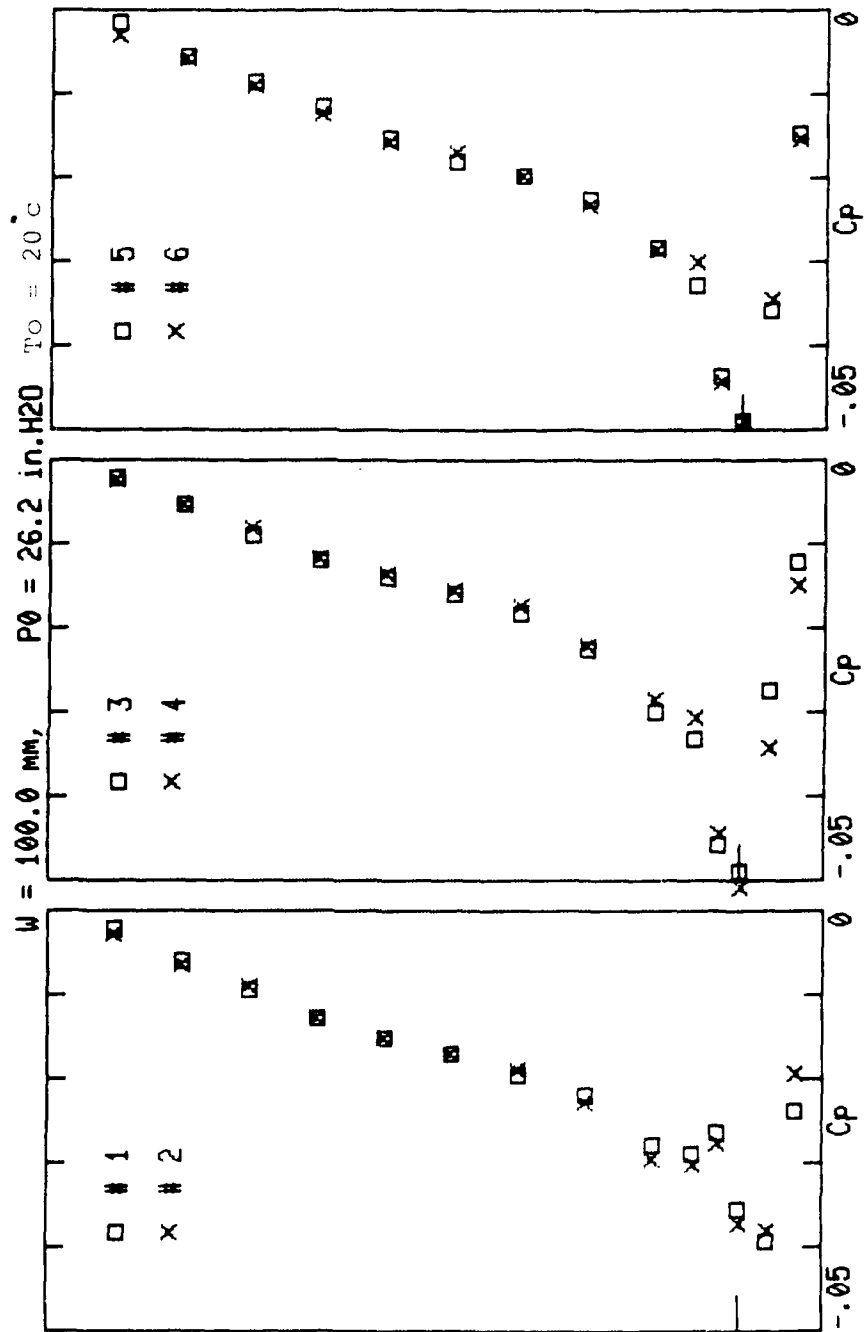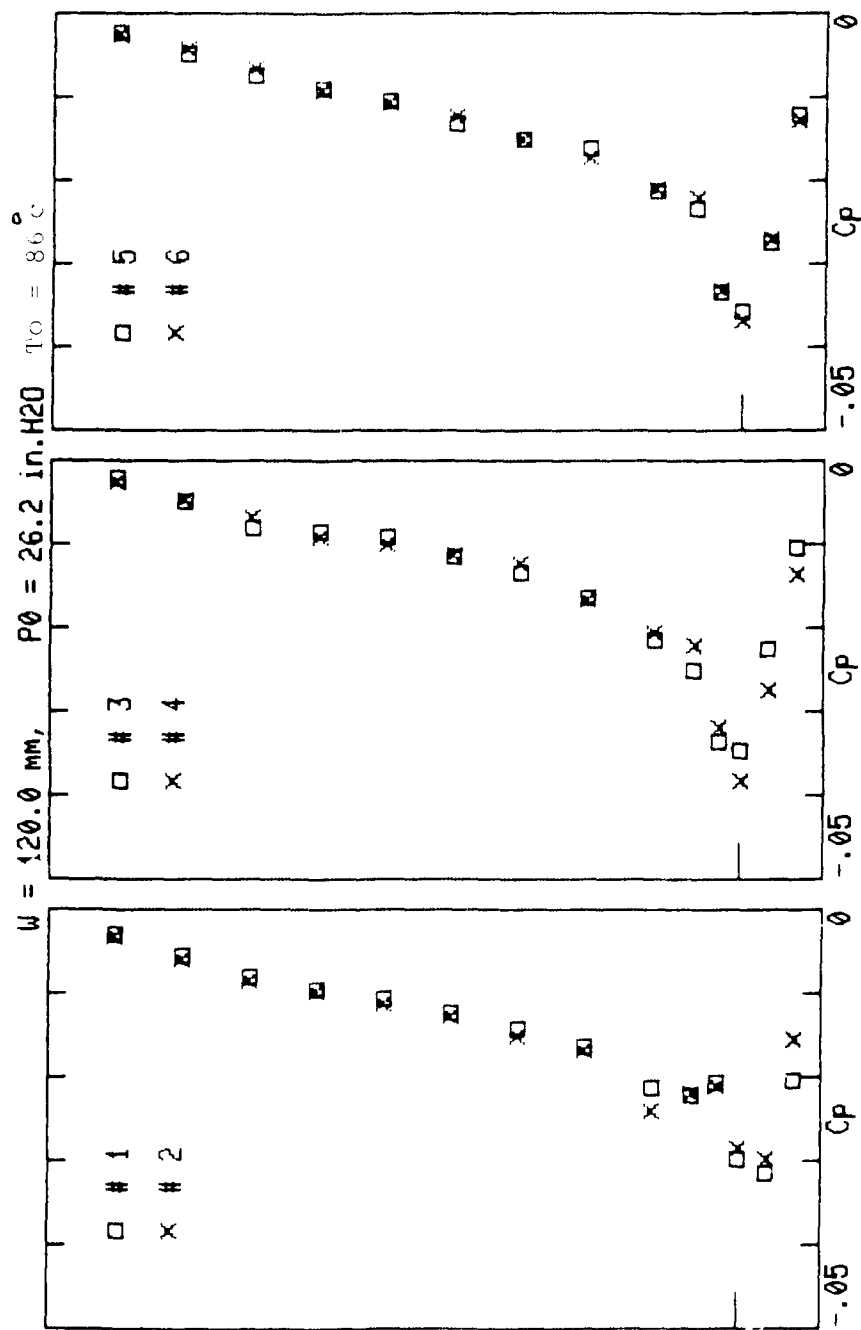
W = 100.0 MM, P0 = 26.2 in.H20 TO = 20°C
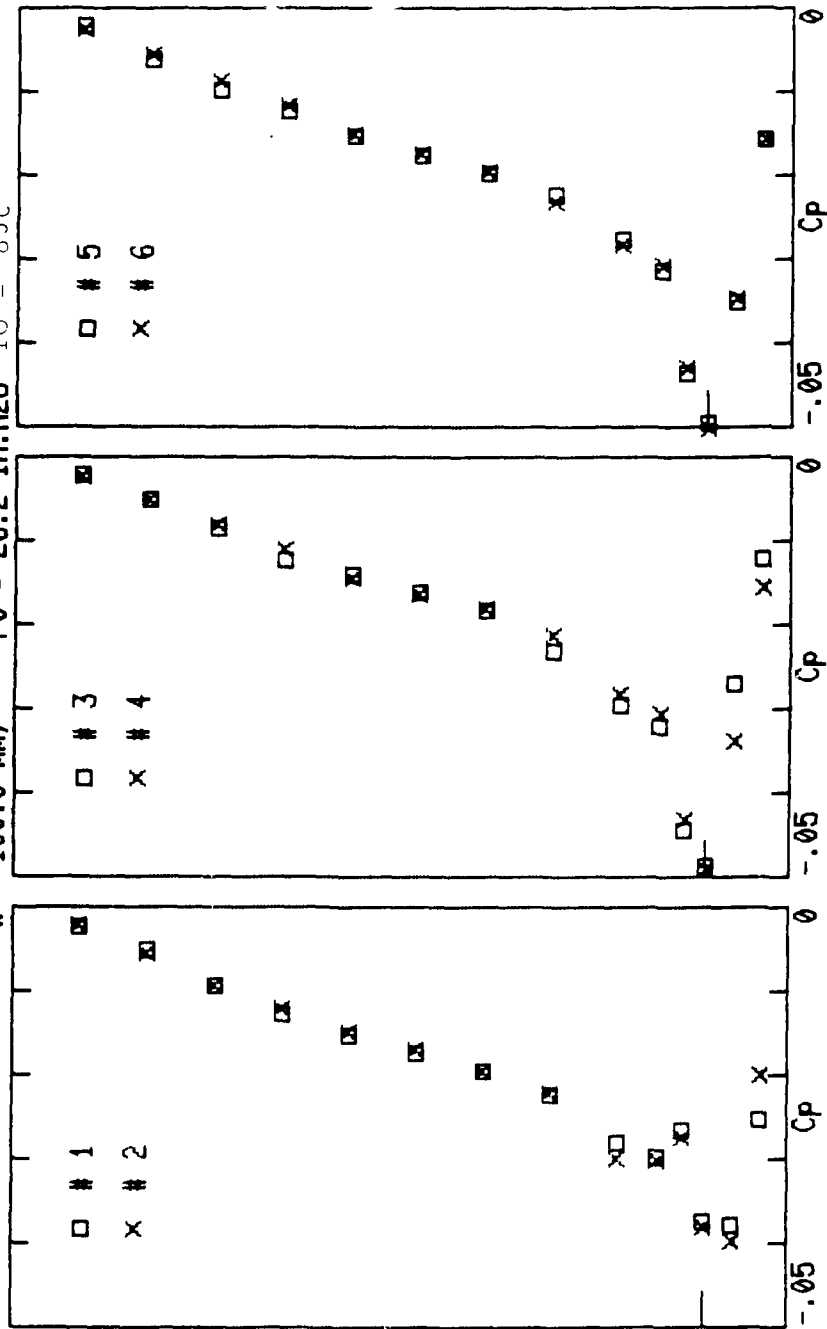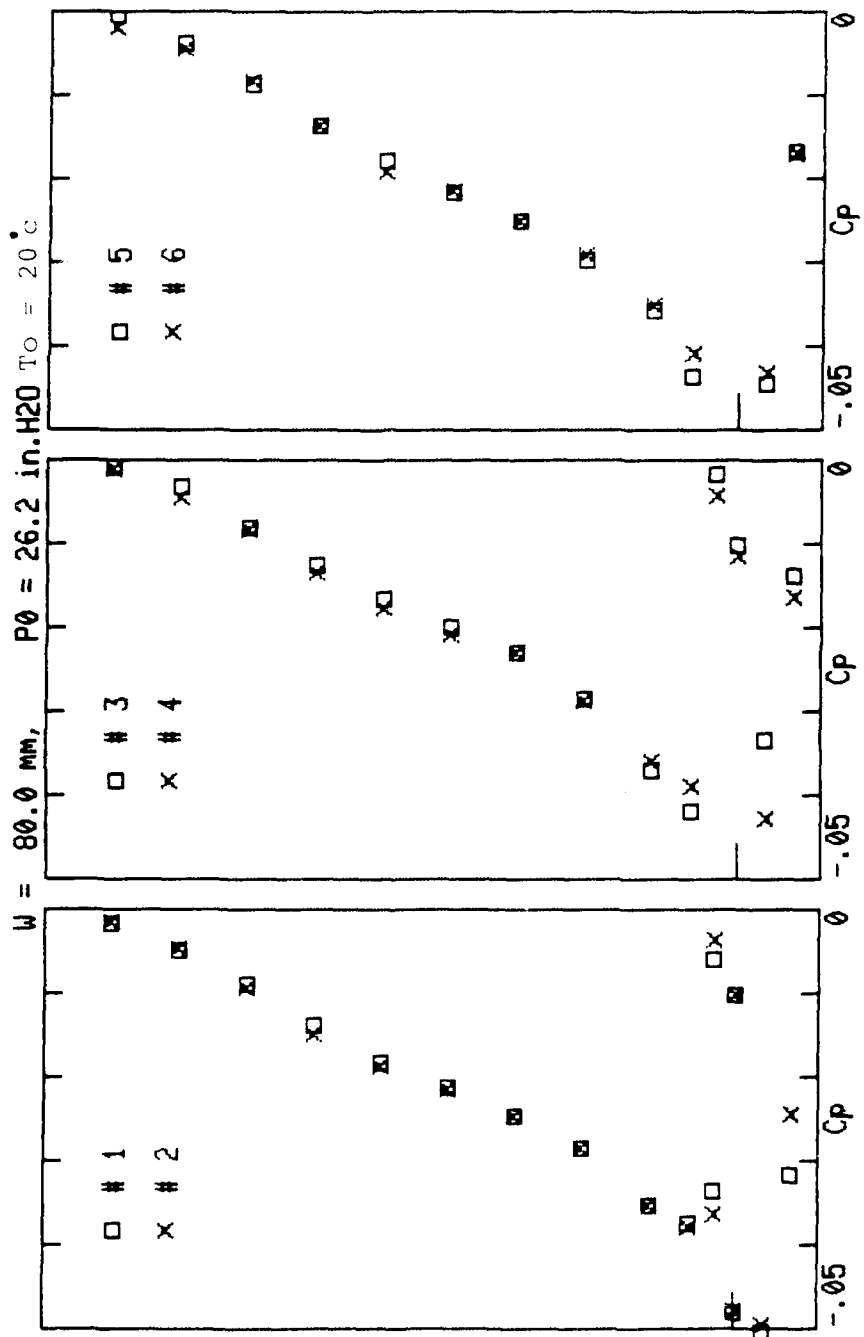
W = 100.0 MM,   PØ = 26.2 in.H2O   To = 85°c

83

W = 80.0 MM, P0 = 26.2 in.H20 T0 = 20°C

84

W = 80.0 mm, P0 = 26.2 in.H2O To = 85°c

W = 120.0 MM,   P0 = 26.2 in.H2O   T0 = 86°C

□ #5   × #6

□ #3   × #4

□ #1   × #2

Cp

Cp

Cp
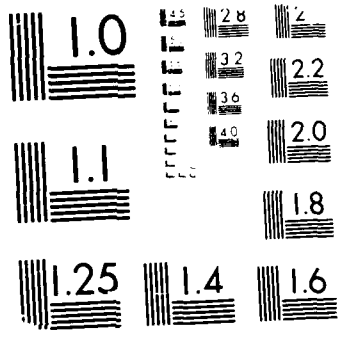
MICROCOPY RESOLUTION TEST CHART

W = 120.0 MM,   P0 = 26.2 in.H2O   To = 85 °C

☆ U.S. GOVERNMENT PRINTING OFFICE 1987 548-054-80581

END
DATE
FILMED
4-88
DTIC